Trilinear Higgs couplings in the two Higgs doublet model with *CP* violation

Per Osland[*]
Department of Physics and Technology, University of Bergen, Postboks 7803, N-5020 Bergen, Norway

P. N. Pandita[+]
Service de Physique Théorique, CEA-Saclay, F-91191 Gif-sur-Yvette Cedex, France

Levent Selbuz[‡]
Department of Physics and Technology, University of Bergen, Postboks 7803, N-5020 Bergen, Norway
(Received 8 February 2008; published 3 July 2008)

We carry out a detailed analysis of the general two Higgs doublet model with *CP* violation. We describe two different parametrizations of this model, and then study the Higgs boson masses and the trilinear Higgs couplings for these two parametrizations. Within a rather general model, we find that the trilinear Higgs couplings have a significant dependence on the details of the model, even when the lightest Higgs boson mass is taken to be a fixed parameter. We include radiative corrections in the one-loop effective potential approximation in our analysis of the Higgs boson masses and the Higgs trilinear couplings. The one-loop corrections to the trilinear couplings of the two Higgs doublet model also depend significantly on the details of the model, and can be rather large. We study quantitatively the trilinear Higgs couplings, and show that these couplings are typically several times larger than the corresponding standard model trilinear Higgs coupling in some regions of the parameter space. We also briefly discuss the decoupling limit of the two Higgs doublet model.

DOI: 10.1103/PhysRevD.78.015003 PACS numbers: 12.60.Fr, 11.30.Er, 14.80.Cp

I. INTRODUCTION

The Higgs mechanism [1] of spontaneous electroweak symmetry breaking is a necessary ingredient of the standard model (SM), which is crucial for its internal consistency. The search for the Higgs boson is, thus, one of the major tasks for the experiments at the upcoming Large Hadron Collider (LHC). In order to confirm the Higgs mechanism as the origin of spontaneous breaking of $SU(2)_L \times U(1)_Y$ gauge symmetry in the SM, not only must the Higgs boson be discovered, but also its trilinear ($\lambda^{\rm SM}_{HHH}$) and quartic ($\lambda^{\rm SM}_{HHHH}$) self-couplings must be measured in order to completely reconstruct the Higgs potential. Furthermore, one must also be able to measure the couplings of the Higgs boson to gauge bosons and fermions.

Here we shall be concerned mainly with the trilinear self-couplings of the Higgs boson. In the standard model, there is only one trilinear self-coupling of the Higgs boson which can be written simply in terms of the Higgs boson mass M_H as

$$\lambda^{\rm SM}_{HHH} = \frac{3M_H^2}{v}, \tag{1.1}$$

where $v = 2M_W/g = 246$ GeV is the vacuum expectation value of the neutral component of the Higgs doublet, M_W is the mass of the $W^{\pm}$, and g is the $SU(2)_L$ gauge coupling, respectively. Several extensions of the SM, such as the minimal supersymmetric standard model (MSSM) [2], and the general two Higgs doublet model (2HDM) [3], have a more complicated Higgs structure. In these models there are several trilinear Higgs couplings, having more complicated dependence on the underlying masses. It is a challenging task to measure [4] these trilinear couplings at the LHC. On the other hand, a linear collider could possibly offer much better prospects of measuring these trilinear Higgs couplings [5–9].

At the proposed International Linear Collider (ILC), if the Higgs boson is not too heavy, the trilinear Higgs coupling can be measured via the Higgs boson pair production $e^+e^- \to W^{+*}\bar{\nu}W^{-*}\nu \to HH\bar{\nu}\nu$. A precise measurement of the trilinear Higgs self-coupling will also make it possible to test extended Higgs models, which have a different structure of the Higgs potential, and hence different trilinear Higgs couplings, as compared to the SM. The 2HDM is the simplest, yet a very general, model with an extended Higgs structure, which leads to various distinct physical effects. In particular, the model can easily accommodate additional *CP* violation [10–13], beyond what is generated by the Kobayashi–Maskawa (KM) mechanism [14]. Furthermore, since there is a distinct possibility of

[*]per.osland@ift.uib.no
[+]ppandita@nehu.ac.in
Permanent address: Department of Physics, North Eastern Hill University, Shillong 793 022, India
[‡]Levent.Selbuz@eng.ankara.edu.tr
Permanent address: Department of Engineering Physics, Faculty of Engineering, Ankara University, 06100 Tandogan-Ankara, Turkey

measuring precisely the Higgs boson self-couplings at the ILC, there is a motivation to study the radiative corrections to the trilinear self-couplings of the Higgs boson.

On the other hand, there are a number of parameters in the potential of the two Higgs doublet model, including those associated with CP violation, which determine the masses and CP properties of the model. In spite of the complicated nature of the Higgs potential, it has been shown in the 2HDM with CP conservation that one-loop corrections to the lightest CP-even Higgs boson self-coupling are in general of a non decoupling nature, and can give rise to $\mathcal{O}(100\%)$ deviations from the SM prediction [15]. This happens even when all other couplings of the lightest Higgs boson to gauge bosons and fermions are in good agreement with the SM prediction.

In this paper we shall study in detail the trilinear Higgs couplings in the two Higgs doublet model with CP violation. We shall assume that the underlying gauge group is the SM gauge group. After spontaneous breaking of the SM gauge symmetry, the Higgs spectrum of the model consists of three neutral Higgs bosons and two charged Higgs bosons. In the CP-conserving version of the model, two neutral Higgs bosons (h^0, H^0) are CP even, whereas one neutral Higgs boson (A^0) is CP odd. In the CP-conserving case, there are, thus, six allowed trilinear Higgs couplings which can be labeled as λ_{hhh}, λ_{hhH}, λ_{hHH}, λ_{HHH} involving the CP-even Higgs bosons, and λ_{hAA}, λ_{HAA}, all even in the number of A^0, involving the CP-odd Higgs boson. When CP is not conserved, the neutral Higgs bosons do not have a definite CP, and there is no such constraint on the couplings involving the A^0 Higgs boson. There are, thus, a total of ten trilinear Higgs couplings in the case of the 2HDM with CP violation.

Since this is one of the simplest models which goes beyond the KM mechanism of CP violation, it is important to study the impact of CP violation on the Higgs self-couplings in this model. We shall, therefore, consider the 2HDM with explicit CP violation in the Higgs sector in this paper. This explicit CP violation is introduced through appropriate complex parameters in the potential of the 2HDM. Furthermore, we shall assume that this explicit CP violation cannot be transformed away by a redefinition of the Higgs fields. Thus, one of the objectives of the present study is to determine the effects of this explicit CP violation in the Higgs sector on various Higgs self-couplings in the two Higgs doublet model. In our study of the model, we shall find it convenient to keep the masses of the two lightest neutral Higgs bosons fixed, and then study the dependence on other parameters of the model, which will determine the amount of explicit CP violation in various Higgs self-couplings, and also determine the mass of the heaviest Higgs boson. In this way, we do not lay emphasis on the heavy Higgs sector of the theory, whereas at the same time we can exhibit the wide range of values that the trilinear Higgs couplings can assume. In particular, we wish to emphasize that, in contrast to the MSSM, the heavy mass effects in a general 2HDM do not decouple. In order to demonstrate this we shall calculate the one-loop corrected Higgs boson self-couplings using the method of effective potential in a general 2HDM with explicit CP violation as described above. This is in contrast to Ref. [15], where all couplings and mass parameters were assumed to be real, thereby precluding the phenomena of explicit CP violation in the Higgs sector as considered in this paper.

The plan of this paper is as follows. In Sec. II we describe the most general two Higgs doublet model with CP violation. We then discuss the spectrum of the Higgs bosons of the model, and the constraints on the parameters when there is CP violation in the model. Here we also discuss how only certain sets of parameters of the Higgs potential can lead to physically consistent models, and discuss different ways in which these parameters can be specified. We delineate the regions of the parameter space where there is no CP violation, corresponding to which one of the neutral Higgs bosons is odd under P. In Sec. III we derive the tree-level trilinear couplings between the neutral as well as the charged Higgs bosons of the model, and discuss the correspondence of these couplings with the trilinear Higgs couplings of the minimal supersymmetric standard model. Here we also study numerically the trilinear Higgs couplings, and discuss the domain of the parameter space that is compatible with various theoretical and experimental constraints.

In Sec. IV we use the method of one-loop effective potential to calculate, as a first step, one-loop corrections to the Higgs boson masses. In Sec. V, we then calculate the one-loop corrections to the trilinear self-couplings of the Higgs bosons. In Sec. VI we carry out a detailed numerical study of the one-loop corrected trilinear Higgs couplings, discuss the magnitudes of different contributions, the dependence on the scale, as well as the decoupling limit, and show that these couplings can be several times larger than the corresponding standard model trilinear Higgs coupling in some regions of the parameter space. We summarize our results and conclusions in Sec. VII. Some of the analytical calculations used in our analysis are described in appendices.

II. THE TWO-HIGGS-DOUBLET MODEL

The general 2HDM with the underlying gauge group $SU(2)_L \times U(1)_Y$ is obtained by extending the Higgs sector of the SM with a second $SU(2)_L$ Higgs doublet with weak hypercharge $Y = 1$. Thus, the model contains 4 complex scalar fields which are arranged as $SU(2)_L$ doublets as follows:

$$\Phi_i = \begin{pmatrix} \varphi_i^+ \\ \varphi_i^0 \end{pmatrix} \quad (Y = +1), \qquad i = 1, 2. \tag{2.1}$$

Using these two Higgs doublets, the most general renor-

malizable potential for the 2HDM which is invariant under the $SU(2)_L \times U(1)_Y$ gauge group can be written as

$$\begin{aligned} V_{\text{tree}} = & \frac{\lambda_1}{2}(\Phi_1^\dagger\Phi_1)^2 + \frac{\lambda_2}{2}(\Phi_2^\dagger\Phi_2)^2 + \lambda_3(\Phi_1^\dagger\Phi_1)(\Phi_2^\dagger\Phi_2) \\ & + \lambda_4(\Phi_1^\dagger\Phi_2)(\Phi_2^\dagger\Phi_1) + \frac{1}{2}[\lambda_5(\Phi_1^\dagger\Phi_2)^2 + \text{H.c.}] \\ & + \{[\lambda_6(\Phi_1^\dagger\Phi_1) + \lambda_7(\Phi_2^\dagger\Phi_2)](\Phi_1^\dagger\Phi_2) + \text{H.c.}\} \\ & - \frac{1}{2}\{m_{11}^2(\Phi_1^\dagger\Phi_1) + [m_{12}^2(\Phi_1^\dagger\Phi_2) + \text{H.c.}] \\ & + m_{22}^2(\Phi_2^\dagger\Phi_2)\}, \end{aligned} \tag{2.2}$$

where $\lambda_i (i = 1, \ldots, 7)$ are dimensionless parameters and the subscript "tree" denotes that (2.2) is a tree-level potential. We note that $\lambda_i (i = 1, \ldots, 4)$ are real, whereas $\lambda_i (i = 5, \ldots, 7)$ are in general complex parameters. Similarly, m_{11}^2 and m_{22}^2 are real, whereas m_{12}^2 is in general complex. We note that the terms proportional to λ_6 and λ_7 have to be constrained, since this potential does not satisfy natural flavor conservation [16], even when each doublet is coupled only to up-type or only to down-type quarks.

When the neutral components of the two Higgs doublets $\Phi_{1,2}$ acquire vacuum expectation values (VEVs), $\varphi_{1,2}^0 = v_{1,2}/\sqrt{2}$, the gauge group $SU(2)_L \times U(1)_Y$ breaks down to $U(1)_{\text{em}}$, whereby three of the eight real fields in (2.1) are absorbed by three of the four gauge bosons of $SU(2)_L \times U(1)_Y$, which become massive in the process, leaving behind a massless photon. We can then parametrize the two Higgs doublet fields in (2.1) as

$$\Phi_i = \begin{pmatrix} \varphi_i^+ \\ \frac{1}{\sqrt{2}}(v_i + \eta_i + i\chi_i) \end{pmatrix}, \qquad i = 1, 2, \tag{2.3}$$

where we have chosen the VEVs of the neutral Higgs fields to be real, and absorbed the relative phase between the two VEVs in the parameters m_{12}^2, λ_5, λ_6 and λ_7 of V_{tree}. When we substitute the parametrization (2.3) of the Higgs fields in the potential (2.2), there will be cubic terms in the Higgs fields arising from the quartic couplings λ_i, which will give rise to trilinear couplings among the Higgs fields. It is these trilinear couplings that we shall study in detail in this paper.

As discussed in the Introduction, in the case of 2HDM with CP conservation, after spontaneous breakdown of the gauge symmetry, we are left with two CP-even Higgs bosons h^0, H^0, a CP-odd Higgs boson A^0, and a pair of charged Higgs bosons $H^\pm$. However, with CP violation the neutral Higgs bosons h^0, H^0, A^0 mix, and it is then more appropriate to define the weak states

$$\begin{pmatrix} \eta_1 \\ \eta_2 \\ \eta_3 \end{pmatrix}, \tag{2.4}$$

to describe the neutral Higgs sector of the CP violating two Higgs doublet model. In (2.4) we have defined

$$\eta_3 = -\sin\beta\chi_1 + \cos\beta\chi_2, \tag{2.5}$$

$$G^0 = \cos\beta\chi_1 + \sin\beta\chi_2, \tag{2.6}$$

where G^0 is the would-be neutral Goldstone boson, and $\tan\beta = v_2/v_1$ is the ratio of the vacuum expectation values of the two Higgs fields. We shall take $\tan\beta$ as an independent parameter. The charged Higgs fields and the corresponding charged Goldstone boson are likewise defined as

$$H^\pm = -\sin\beta\varphi_1^\pm + \cos\beta\varphi_2^\pm, \tag{2.7}$$

$$G^\pm = \cos\beta\varphi_1^\pm + \sin\beta\varphi_2^\pm, \tag{2.8}$$

respectively.

A. Basis rotation

The tree-level mass squared matrix of the neutral Higgs bosons can now be defined as

$$\mathcal{M}^2_{ij} = \frac{\partial^2 V}{\partial\eta_i\partial\eta_j}, \tag{2.9}$$

where, after differentiation, all fields are set equal to zero: $\eta_1 = \eta_2 = \eta_3 = H^\pm = G^0 = G^\pm = 0$. The physical neutral Higgs states H_i, which are the eigenstates of the mass squared matrix (2.9), are then obtained by a rotation R

$$H = R\eta, \qquad \eta = R^{\text{T}}H, \tag{2.10}$$

or, more explicitly

$$H_i = R_{ij}\eta_j, \qquad \eta_j = R_{ij}H_i. \tag{2.11}$$

The rotation matrix R which diagonalizes (2.9),

$$R\mathcal{M}^2R^{\text{T}} = \mathcal{M}^2_{\text{diag}} = \text{diag}(M_1^2, M_2^2, M_3^2), \tag{2.12}$$

with $M_1 < M_2 < M_3$, can be parametrized as

$$\begin{aligned} R &= R_3R_2R_1 \\ &= \begin{pmatrix} 1 & 0 & 0 \\ 0 & \cos\alpha_3 & \sin\alpha_3 \\ 0 & -\sin\alpha_3 & \cos\alpha_3 \end{pmatrix}\begin{pmatrix} \cos\alpha_2 & 0 & \sin\alpha_2 \\ 0 & 1 & 0 \\ -\sin\alpha_2 & 0 & \cos\alpha_2 \end{pmatrix} \\ &\quad \times \begin{pmatrix} \cos\alpha_1 & \sin\alpha_1 & 0 \\ -\sin\alpha_1 & \cos\alpha_1 & 0 \\ 0 & 0 & 1 \end{pmatrix} \\ &= \begin{pmatrix} c_1c_2 & s_1c_2 & s_2 \\ -(c_1s_2s_3 + s_1c_3) & c_1c_3 - s_1s_2s_3 & c_2s_3 \\ -c_1s_2c_3 + s_1s_3 & -(c_1s_3 + s_1s_2c_3) & c_2c_3 \end{pmatrix}, \end{aligned} \tag{2.13}$$

where $c_i = \cos\alpha_i$, $s_i = \sin\alpha_i$. Note that Eq. (2.12) can be inverted as

$$(\mathcal{M}^2)_{ij} = \sum_k R_{ki}M_k^2R_{kj}. \tag{2.14}$$

By symmetry, $(\mathcal{M}^2)_{ji} = (\mathcal{M}^2)_{ij}$, and, in the general case,

this matrix is seen to contain 6 independent parameters. These may be taken as the three masses, and the angles of the rotation matrix.

As discussed in Ref. [17], there are three limits in which there is no CP violation in the 2HDM, corresponding to which one of the neutral Higgs bosons is odd under P. These limits can be characterized in terms of the angles α_2 and α_3 of the rotation matrix (2.13) as follows:

$$H_1 \text{ is odd: } \alpha_2 = \pm\pi/2, \tag{2.15}$$

$$H_2 \text{ is odd: } \alpha_3 = \pm\pi/2, \tag{2.16}$$

$$H_3 \text{ is odd: } \alpha_2 = 0, \qquad \alpha_3 = 0. \tag{2.17}$$

We note that in the latter limit, we have $\alpha_1 = \alpha + \pi/2$, where α is the conventional mixing angle in the CP-even sector of the MSSM [3]. Any CP violation in the 2HDM will also depend on the Yukawa couplings. In the 2HDM II (Model II), where the down-type quarks couple to Φ_1 and the up-type quarks couple to Φ_2, various measures of "maximal" CP violation both in the Higgs-vector boson and Higgs-quark sectors are discussed in [18]. These maxima occur in the "bulk" of the α_2–α_3 space, typically for $|\alpha_2| = \mathcal{O}(\pi/4)$ and $|\alpha_3| = \mathcal{O}(\pi/4)$.

B. Neutral Higgs boson masses

Minimizing the tree-level potential according to

$$\frac{\partial V}{\partial \Phi_i} = 0, \quad i = 1, 2, \tag{2.18}$$

and using the resulting minimization conditions to eliminate m_{11}^2 and m_{22}^2, one obtains the elements (2.9) of the tree-level mass squared matrix

$$\begin{aligned}
\mathcal{M}_{11}^2 &= v_1^2\lambda_1 + v_2^2\nu + \frac{v_2}{2v_1}\,\mathrm{Re}(3v_1^2\lambda_6 - v_2^2\lambda_7),\\
\mathcal{M}_{22}^2 &= v_2^2\lambda_2 + v_1^2\nu + \frac{v_1}{2v_2}\,\mathrm{Re}(-v_1^2\lambda_6 + 3v_2^2\lambda_7),\\
\mathcal{M}_{33}^2 &= v^2\,\mathrm{Re}\Big[-\lambda_5 + \nu - \frac{1}{2v_1v_2}(v_1^2\lambda_6 + v_2^2\lambda_7)\Big],\\
\mathcal{M}_{12}^2 &= v_1v_2[\mathrm{Re}(\lambda_3 + \lambda_4 + \lambda_5) - \nu]\\
&\quad + \frac{3}{2}\,\mathrm{Re}(v_1^2\lambda_6 + v_2^2\lambda_7),\\
\mathcal{M}_{13}^2 &= -\frac{1}{2}v\,\mathrm{Im}[v_2\lambda_5 + 2v_1\lambda_6],\\
\mathcal{M}_{23}^2 &= -\frac{1}{2}v\,\mathrm{Im}[v_1\lambda_5 + 2v_2\lambda_7],
\end{aligned} \tag{2.19}$$

where we have defined

$$v_1 = v\cos\beta, \qquad v_2 = v\sin\beta, \qquad \beta \in \Big(0, \frac{\pi}{2}\Big), \tag{2.20}$$

and

$$\nu = \frac{1}{2v_1v_2}\,\mathrm{Re}(m_{12}^2), \tag{2.21}$$

with $v^2 = v_1^2 + v_2^2 = (246\ \mathrm{GeV})^2$. The squared masses M_i^2 of the physical neutral Higgs bosons are obtained as the eigenvalues of the mass squared matrix (2.9). These eigenvalues are solutions of a cubic equation which involves the parameters λ_i. However, only some set of values of the parameters λ_i lead to consistent solutions. In order to identify physically consistent models, we shall, following the approach of Refs. [19–21], specify physical (tree-level) masses, instead of the λ_i, as parameters. Depending on how much constrained a model we want to consider, we shall do this in two ways, which we shall denote "approach (A)" and "approach (B)":

(A) In this case, which corresponds to $\lambda_6 = \lambda_7 = 0$, two elements of $\mathcal{M}^2$ are related via $\tan\beta$ and we cannot therefore take all three masses as independent. Instead, we take the *two lightest* neutral Higgs boson masses, together with $\tan\beta$ and the three angles (α_1, α_2, α_3) defining the mixing matrix R of Eq. (2.10), as independent parameters. The third (heaviest) Higgs boson mass can then readily be determined. In general, the elements R_{13} and R_{23} of the rotation matrix R must be nonzero in order to have CP violation. For consistency, the derived quantities $\mathrm{Im}\lambda_5$ and $\mathrm{Im}\,m_{12}^2$ must be nonzero.

(B) Here we take λ_6, $\lambda_7 \neq 0$. In this case, we take all *three* neutral Higgs boson masses, $\tan\beta$, together with the mixing matrix R of Eq. (2.10), $\mathrm{Im}\lambda_5$, $\mathrm{Re}\lambda_6$, and $\mathrm{Re}\lambda_7$ as the input parameters.

In either case, specifying the charged Higgs boson mass, $M_{H^\pm}$, as well as the bilinear parameter $\mu^2 = v^2\nu$, we can determine the remaining λ_i through a set of linear relations. They are, thus, unique. Details are given in Appendix A.

We note that in general, there exist multiple minima in the 2HDM potential [10,22]. However, with our choice of input parameters, including Higgs squared masses, and these being positive, the minimum we are working in is a global one and hence stable [23].

III. TRILINEAR SELF-COUPLINGS OF HIGGS BOSONS AT THE TREE LEVEL

In this Section we shall define the trilinear Higgs self-couplings, and obtain explicit expressions for them in terms of the parameters of the tree-level Higgs potential of the 2HDM. We shall then study the behavior of these couplings as functions of the various parameters of the model.

A. Trilinear couplings of neutral Higgs bosons

The trilinear self-couplings of the neutral Higgs bosons are defined as

$$\lambda_{ijk} = \frac{-i\partial^3 V}{\partial H_i \partial H_j \partial H_k}, \tag{3.1}$$

which are most easily obtained from the corresponding derivatives of V in (2.2) with respect to the weak fields η_ℓ. The derivatives with respect to H_i in (3.1) are obtained by noting the useful relation

$$\frac{\partial}{\partial H_i} = \frac{d\eta_j}{dH_i}\frac{\partial}{\partial \eta_j} = R_{ij}\frac{\partial}{\partial \eta_j}, \tag{3.2}$$

which can be used to go from the η_i basis to the physical H_i basis.

When there is CP violation, the trilinear couplings among the physical Higgs bosons will involve elements of the rotation matrix R [24,25]. We can then write the trilinear couplings in terms of the derivatives of the potential (2.2) with respect to η_ℓ and the elements of the rotation matrix R as

$$\begin{aligned}\lambda_{ijk} &= \sum_{m\le n\le o=1,2,3}^{*} R_{i'm}R_{j'n}R_{k'o}\frac{-i\partial^3 V}{\partial\eta_m\partial\eta_n\partial\eta_o} \\ &= \sum_{m\le n\le o=1,2,3}^{*} R_{i'm}R_{j'n}R_{k'o}a_{mno},\end{aligned} \tag{3.3}$$

where the indices m, n, o refer to the weak field basis, and the $*$ denotes a sum over permutations $P, \{i', j', k'\} = P\{i, j, k\}$, which gives rise to a factor of $n!$ for n identical fields. We now proceed to obtain these couplings in an explicit form.

At the tree level, when expressed in terms of λ_i, the derivatives in Eq. (3.3) are rather simple. The trilinear couplings a_{mno} among the weak fields η_ℓ can be written as (in units of $-iv$) [24,25]:

$$\begin{aligned}
a_{111} &= \tfrac{1}{2}(\cos\beta\lambda_1 + \sin\beta\,\mathrm{Re}\lambda_6),\\
a_{112} &= \tfrac{1}{2}(\sin\beta\,\mathrm{Re}\lambda_{345} + 3\cos\beta\,\mathrm{Re}\lambda_6),\\
a_{113} &= -\tfrac{1}{2}[\cos\beta\sin\beta\,\mathrm{Im}\lambda_5 + (1+2\cos^2\beta)\,\mathrm{Im}\lambda_6],\\
a_{122} &= \tfrac{1}{2}(\cos\beta\,\mathrm{Re}\lambda_{345} + 3\sin\beta\,\mathrm{Re}\lambda_7),\\
a_{123} &= -\mathrm{Im}\lambda_5 - \cos\beta\sin\beta(\mathrm{Im}\lambda_6 + \mathrm{Im}\lambda_7),\\
a_{133} &= \tfrac{1}{2}\{\cos\beta(\sin^2\beta\lambda_1 + \cos^2\beta\,\mathrm{Re}\lambda_{345} - 2\,\mathrm{Re}\lambda_5)\\
&\quad + \sin\beta[(\sin^2\beta - 2\cos^2\beta)\,\mathrm{Re}\lambda_6 + \cos^2\beta\,\mathrm{Re}\lambda_7]\},\\
a_{222} &= \tfrac{1}{2}(\sin\beta\lambda_2 + \cos\beta\,\mathrm{Re}\lambda_7),\\
a_{223} &= -\tfrac{1}{2}[\cos\beta\sin\beta\,\mathrm{Im}\lambda_5 + (\cos^2\beta + 3\sin^2\beta)\,\mathrm{Im}\lambda_7],\\
a_{233} &= \tfrac{1}{2}\{\sin\beta(\cos^2\beta\lambda_2 + \sin^2\beta\,\mathrm{Re}\lambda_{345} - 2\,\mathrm{Re}\lambda_5)\\
&\quad + \cos\beta[\sin^2\beta\,\mathrm{Re}\lambda_6 + (\cos^2\beta - 2\sin^2\beta)\,\mathrm{Re}\lambda_7]\},\\
a_{333} &= \tfrac{1}{2}(\cos\beta\sin\beta\,\mathrm{Im}\lambda_5 - \sin^2\beta\,\mathrm{Im}\lambda_6 - \cos^2\beta\,\mathrm{Im}\lambda_7),
\end{aligned} \tag{3.4}$$

where

$$\lambda_{345} = \lambda_3 + \lambda_4 + \lambda_5. \tag{3.5}$$

In order to elucidate the compact notation in Eq. (3.3), we explicitly write the trilinear couplings λ_{111} and λ_{112} in Appendix B.

Rather than studying all the trilinear couplings of the Higgs bosons, we shall here focus on the two couplings λ_{111} and λ_{112} involving the lightest Higgs boson H_1. In the special case when $\lambda_6 = \lambda_7 = 0$, and if in addition $\alpha_2 = \alpha_3 = 0$, these couplings take the simple form

$$\begin{aligned}\lambda_{111} &= -3iv\{c_1^3 c_\beta\lambda_1 + s_1^3 s_\beta\lambda_2\\ &\quad + c_1 s_1(c_1 s_\beta + s_1 c_\beta)\,\mathrm{Re}\lambda_{345}\},\end{aligned} \tag{3.6a}$$

$$\begin{aligned}\lambda_{112} &= iv\{3c_1 s_1(c_1 c_\beta\lambda_1 - s_1 s_\beta\lambda_2)\\ &\quad - [c_1^3 s_\beta - s_1^3 c_\beta + 2c_1 s_1(c_1 c_\beta - s_1 s_\beta)]\\ &\quad \times \mathrm{Re}\lambda_{345}\}.\end{aligned} \tag{3.6b}$$

In this limit of $\lambda_6 = \lambda_7 = 0$ and $\alpha_2 = \alpha_3 = 0$, we note the following:

(i) For small values of $\tan\beta$, both λ_{111} and λ_{112} are determined by λ_1 and $\mathrm{Re}\lambda_{345}$. This is because for small $\tan\beta$, terms containing $s_\beta \equiv \sin\beta$ vanish. In actual practice, due to the constraints imposed by B-physics, the small $\tan\beta$ limit is not reached.

(ii) For large values of $\tan\beta$, both λ_{111} and λ_{112} are determined by λ_2 and $\mathrm{Re}\lambda_{345}$. In this case terms containing $c_\beta \equiv \cos\beta$ vanish.

Here, the combination $\mathrm{Re}\lambda_{345}$ is related to $M_{H^\pm}^2$ via

$$M_{H^\pm}^2 = \mu^2 + \tfrac{1}{2}v^2[\lambda_3 - \mathrm{Re}\lambda_{345} - \mathrm{Re}(\lambda_6 + \lambda_7)]. \tag{3.7}$$

It is instructive to compare the couplings (3.6) with the standard model trilinear coupling (1.1). While the SM trilinear coupling is given in terms of only one parameter, the mass M_H of the Higgs boson, those of the 2HDM depend on several parameters, and may actually pass through zero, even for the special case studied in Eq. (3.6). In the general case, we find it convenient to study the dimensionless ratios of the couplings

$$\xi_1 \equiv \frac{\lambda_{111}}{\lambda_{HHH}^{\mathrm{SM}}}, \qquad \xi_2 \equiv \frac{\lambda_{112}}{\lambda_{HHH}^{\mathrm{SM}}}, \tag{3.8}$$

where for the reference SM coupling we use the mass M_1 of the lightest Higgs boson of the 2HDM. These dimensionless ratios of the couplings will be calculated and discussed in the following.

1. 2HDM–MSSM correspondence

It is also useful to compare the trilinear Higgs couplings in the 2HDM with the corresponding ones in the minimal supersymmetric standard model. In the MSSM, where there is no CP violation in the Higgs sector at the tree level, there are six trilinear Higgs couplings. The couplings corresponding to λ_{111} and λ_{112} are [6,26]

$$\lambda_{hhh} = -\frac{3igM_Z}{2\cos\theta_W}\cos(2\alpha)\sin(\alpha+\beta), \tag{3.9a}$$

$$\lambda_{hhH} = -\frac{igM_Z}{2\cos\theta_W}[2\sin(2\alpha)\sin(\alpha+\beta) - \cos(2\alpha)\cos(\alpha+\beta)], \tag{3.9b}$$

where M_Z is the mass of the Z, θ_W is the Weinberg angle, and g the $SU(2)_L$ gauge coupling. The angle α is the mixing angle in the CP even Higgs sector of the MSSM. In the limit $\alpha_2 \to 0$ and $\alpha_3 \to 0$, it corresponds to $\alpha_1 - \pi/2$ of the 2HDM.

In the MSSM the trilinear Higgs couplings are controlled by the $SU(2)_L$ gauge coupling g. In contrast, the trilinear Higgs couplings in the 2HDM arise from the quartic terms of the Higgs potential when the SM gauge symmetry is broken. It is easy to see that in the above limit the couplings in the two models are simply related by the following correspondence

$$\lambda_1 = \lambda_2 \leftrightarrow \tfrac{1}{4}(g^2+g'^2), \qquad \mathrm{Re}\lambda_{345} \leftrightarrow -\tfrac{1}{4}(g^2+g'^2), \tag{3.10}$$

together with

$$\lambda_6 = \lambda_7 = 0, \tag{3.11}$$

where g' is the $U(1)$ hypercharge coupling. We note that the constraint (3.11) is accessible in approach (A), but not in (B). Using this correspondence, together with $\alpha_1 \to \alpha + \pi/2$ and

$$\frac{1}{4}(g^2+g'^2)v = \frac{gM_Z}{2\cos\theta_W}, \tag{3.12}$$

we find

$$\lambda_{111} \leftrightarrow \lambda_{hhh}, \qquad \lambda_{112} \leftrightarrow \lambda_{hhH}. \tag{3.13}$$

For the relations (3.10) to be satisfied, one needs the nontrivial relations

$$\lambda_1 = \lambda_2 = -\mathrm{Re}\lambda_{345}. \tag{3.14}$$

When (3.11) holds, and

$$\alpha_2 = \alpha_3 = 0, \tag{3.15}$$

then (more general relations can be found in Appendix A)

$$\lambda_1 = \frac{1}{c_\beta^2 v^2}[c_1^2 M_1^2 + s_1^2 M_2^2 - s_\beta^2 \mu^2],$$

$$\lambda_2 = \frac{1}{s_\beta^2 v^2}[s_1^2 M_1^2 + c_1^2 M_2^2 - c_\beta^2 \mu^2], \tag{3.16}$$

$$\mathrm{Re}\lambda_{345} = \frac{1}{c_\beta s_\beta v^2} c_1 s_1 (M_1^2 - M_2^2) + \frac{\mu^2}{v^2}.$$

We note that Eq. (3.14) can be satisfied when $\alpha_1 \simeq \beta \simeq \pi/4$ and M_2 and μ are both large compared to M_1:

$$\frac{\sin 2\alpha_1}{\sin 2\beta} = \frac{M_2^2 + M_1^2}{M_2^2 - M_1^2}. \tag{3.17}$$

In this limit,[1] the 2HDM will correspond to the Higgs sector of the CP-conserving MSSM. In fact, since the two potentials in this limit will be the same, the other trilinear couplings in the two models will also be identical in this limit.

We note that the MSSM couplings (3.9), like those of the 2HDM, vanish for certain choices of the mixing angles α and β. The exact values of parameters where they vanish will be modified when radiative corrections are taken into account. However, the modifications will be only quantitative in nature.

As a special case of the limit of no CP violation discussed above, we note that the MSSM Higgs couplings possess an additional important property, which is usually referred to as decoupling [27]. This property can be described as follows. If $M_{A^0} \gg M_Z$, then $\alpha \to \beta - \pi/2$ and the coupling λ_{hhh} approaches $\lambda_{HHH}^{\mathrm{SM}}$ [28,29]. It follows that in this limit, which is called the decoupling limit, $\xi_1 \to 1$. In the present notation, this requires $\alpha_1 \simeq \beta$, with $M_2 \simeq \mu$. (However, the correspondence between the 2HDM and the MSSM described above fails for $\tan\beta$ away from unity.) We will return to the issue of decoupling in Sec. VI C.

2. Numerical study

For fixed values of the Higgs boson masses, only a small domain in the parameter space of $\boldsymbol{\alpha} = (\alpha_1, \alpha_2, \alpha_3)$ is compatible with positivity [20,30], and the perturbative unitarity in the Higgs sector [31–33]. Furthermore, there are experimental constraints from B physics: $B \to X_s\gamma$ [34–36], $B \to \tau\bar{\nu}_\tau$ [37,38], and B–$\bar{B}$ oscillations [35,39]. These do not depend on details of the neutral Higgs sector, but since these processes can get contributions from $H^\pm$ exchange, they constrain the allowed values of $\tan\beta$ and $M_{H^\pm}$. Furthermore, there are experimental constraints that do depend on the neutral Higgs sector. These are R_b [40,41], nonobservation of a light neutral Higgs boson at LEP [40], and most importantly the constraint arising [20,42,43] from $\Delta\rho$ [44]. In contrast to the case of the MSSM, $(g-2)$ does not play any important role here. The experimental constraints on the Higgs sector of the 2HDM are discussed in [17]. Here we shall follow the same approach, defining a χ^2 function

$$\chi^2(\boldsymbol{\alpha}) = \chi^2_{\mathrm{general}} + \sum_i \chi_i^2(\boldsymbol{\alpha}), \tag{3.18}$$

where the first term, which is independent of $\boldsymbol{\alpha}$, is due to various B-physics constraints, $\bar{B} \to X_s\gamma$, $B^- \to \tau\bar{\nu}_\tau$ and B–$\bar{B}$ oscillations

[1] With $c_\beta^2 = \frac{1}{2} + \epsilon$, one finds to lowest order in ϵ: $c_1^2 = \frac{1}{2} + \epsilon(2\mu^2/M_2^2 - 1)$ and $M_1^2 = 2\epsilon^2(M_2^2 + \mu^2 - 2\mu^4/M_2^2)$.

$$\chi^2_{\rm general} = \chi^2_{b\to s\gamma} + \chi^2_{b\to\tau\nu} + \chi^2_{B-\bar{B}}, \tag{3.19}$$

and the second term is a sum over contributions due to observables $\mathcal{O}_i$ that depend on $\boldsymbol{\alpha}$. These are the nonobservation of a light neutral Higgs boson at LEP2, the $Z^0 \to b\bar{b}$ decay rate, and $\Delta\rho$:

$$\chi^2_i(\boldsymbol{\alpha}) = \frac{(\mathcal{O}_{i,\rm 2HDM}(\boldsymbol{\alpha}) - \mathcal{O}_{i,\rm ref})^2}{[\sigma(\mathcal{O}_i)]^2}. \tag{3.20}$$

We adopt the same definitions and experimental data as were used in [17], allowing parameters for which $\chi^2 \leq 5.99$, corresponding to a 95% C.L.

Some of the main features of these constraints are worth stressing. First of all, for small values of μ^2, the allowed range of $\tan\beta$ is restricted by unitarity to values below 5–8 [17]. Second, for large values of $M_{H^\pm}$, the $\Delta\rho$ constraint requires $M_2 \sim M_3 \sim M_{H^\pm}$, especially for large values of $\tan\beta$ [21].

Within an allowed domain in the parameter space, the trilinear couplings can have a very strong dependence on the neutral Higgs boson mixing angles, as is illustrated in Fig. 1, where we have plotted ξ_1 as a function of α_1, keeping $\alpha_2 = \pm\pi/4$ and $\alpha_3 = \pi/12$ fixed.

In this figure, the values of the trilinear coupling are calculated at tree level with $M_1 = 120$ GeV, $\mu = 0$, $\tan\beta = 1$, $\alpha_2 = \pm\pi/4$, and $\alpha_3 = \pi/12$. The upper set of lines in this figure (larger values of the trilinear couplings) refer to the approach (A) of Sec. II B, where we take

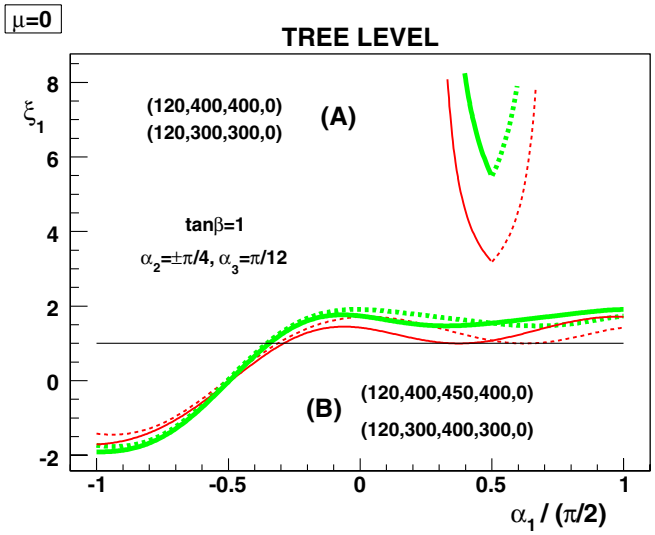

FIG. 1 (color online). The trilinear coupling ratio ξ_1 defined in (3.8) at the tree level plotted as a function of α_1 for both the approaches (A) and (B), for two different values of α_2 ($-\pi/4$, dashed line, and $+\pi/4$, solid line), both with $\alpha_3 = \pi/12$. The masses of the Higgs bosons are $M_1 = 120$ GeV, with $M_2 = M_{H^\pm} = 300$ GeV (red, thin lines), and $M_2 = M_{H^\pm} = 400$ GeV (green, heavy lines). Furthermore, $\mu = 0$ and $\tan\beta = 1$. The numbers in insets give values of $(M_1, M_2, M_{H^\pm}, \mu)$ for approach (A) and for those of $(M_1, M_2, M_3, M_{H^\pm}, \mu)$ for approach (B).

$\lambda_6 = \lambda_7 = 0$, and fix $M_2 = M_{H^\pm} = 300$ GeV, or $M_2 = M_{H^\pm} = 400$ GeV, as indicated in the caption. The lower set of lines refer to the approach (B), where we fix $(M_2, M_3, M_{H^\pm})$ equal to (300, 400, 300) GeV, or (400, 450, 400) GeV, with the additional constraints $\mathrm{Im}\lambda_5 = 0$, $\mathrm{Re}\lambda_6 = \mathrm{Re}\lambda_7 = 0$.

From this figure we note a marked qualitative difference between the values of the trilinear coupling calculated via the two approaches of specifying the input parameters. In general, they both lead to solutions for only limited ranges of α_1, keeping M_3 fixed [approach (B)], the variation of the coupling with α_1 is modest, whereas when $\lambda_6 = \lambda_7 = 0$ and M_3 is calculated [approach (A)], the variation with α_1 is quite strong (upper part of the figure).

The different behavior of the trilinear coupling in the two approaches can be understood as follows. The trilinear couplings are linear functions of the quartic couplings λ_i in the Higgs potential (2.2). In both the approaches, (A) and (B), the couplings λ_i are rather smooth functions of α_1. They are also comparable in magnitude, with the exception that in approach (B), where we fix M_3, we also take as input $\mathrm{Im}\lambda_5 = 0$. Thus, the role played by $\mathrm{Im}\lambda_5$ in approach (A) is played by $\mathrm{Im}\lambda_6$ and $\mathrm{Im}\lambda_7$ in approach (B). This switch of role from $\mathrm{Im}\lambda_5$ to $\mathrm{Im}\lambda_6$ and $\mathrm{Im}\lambda_7$ has as a consequence, for the case studied in Fig. 1, that a_{333} (which is quite large) switches sign. Since the coefficient in (3.3) that relates a_{333} to λ_{111} is essentially R^3_{13}, with $R_{13} = \sin\alpha_2 = \pm 1/\sqrt{2}$, this sign change of the large coupling a_{333} is the dominant effect which causes the difference between the parameter choices in the approaches (A) and (B) (for the set of parameters considered). In fact, truncating Eq. (3.3) with $a_{333} = 0$, one finds the ratio of the couplings $\xi_1 = 3.8$–5 for approach (A), and 3.6–3.8 for approach (B), where we have taken $M_1 = 120$ GeV, $M_2 = 400$ GeV, $\alpha_2 = -\pi/4$, and $\alpha_3 = \pi/12$ for both the approaches. Thus, one may conclude that the two different ways of introducing CP violation in the two Higgs doublet model lead to very different values for the trilinear coupling λ_{111}.

Furthermore, we note that $\mathrm{Re}\lambda_5$ depends on α_1 through M_3 only [17]. Thus, in approach (A), with M_3 depending on α_1, the resulting $\mathrm{Re}\lambda_5$ will also vary, whereas in approach (B), $\mathrm{Re}\lambda_5$ is constant. This contributes to the stronger variation of ξ_1 with α_1 in approach (A).

In view of the strong dependence of the trilinear couplings on the mixing angles, we shall henceforth average over these angles within the allowed ranges. In Figs. 2 and 3 we show the tree-level ratios

$$\langle\xi_1\rangle = \frac{\langle\lambda_{111}\rangle}{\lambda^{\rm SM}_{HHH}}, \qquad \langle\xi_2\rangle = \frac{\langle\lambda_{112}\rangle}{\lambda^{\rm SM}_{HHH}}, \tag{3.21}$$

for a representative choice of parameter sets. These are *averages*, obtained by scanning over the $\boldsymbol{\alpha} = (\alpha_1, \alpha_2, \alpha_3)$ space, subjecting all model points to positivity, unitarity, and the experimental constraints discussed above, working within the approach (A) defined in Sec. II B, and normal-

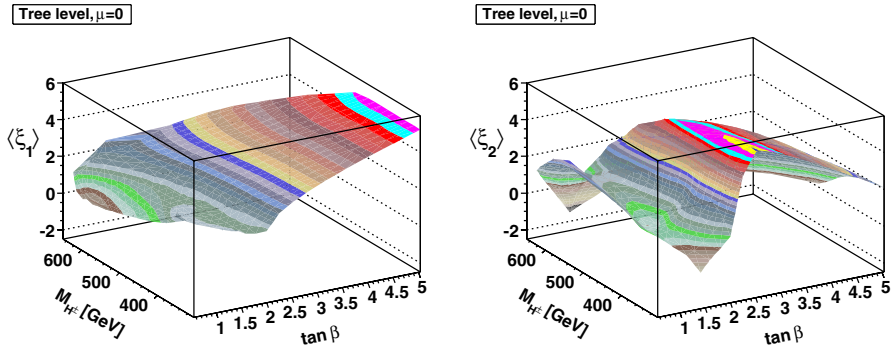

FIG. 2 (color online). Trilinear Higgs coupling ratios $\langle\xi_1\rangle$ and $\langle\xi_2\rangle$ as defined in Eq. (3.21) at the tree level, in approach (A), for the values of the Higgs masses $M_1 = 120$ GeV, $M_2 = 300$ GeV, and $\mu = 0$. The ratios are plotted for the case of the CP-conserving MSSM-like limit as defined in Eq. (3.22).

izing them with respect to the SM coupling, as defined in Eq. (3.8). The scans are performed over $200 \times 200 \times 100$ points.

Before considering the general case of arbitrary CP violation, we first consider, in Fig. 2, a region of parameter space near the limit (2.17) of no CP violation:

$$|\alpha_2| \leq \alpha_0, \qquad |\alpha_3| \leq \alpha_0, \qquad \alpha_0 = 0.05 \times \pi/2, \tag{3.22}$$

referred to as "*minimal CP violation.*" From the above discussion [see Eqs. (3.10), (3.11), (3.12), and (3.13)], it follows that this corresponds to a domain of parameters close to the CP-conserving Higgs sector of the MSSM. We note that the approach (A), where we determine M_3 from M_1, M_2 and the rotation matrix, does not permit us to go all the way to the limit $\alpha_2 = \alpha_3 = 0$.

In this figure, which is valid for $\mu = 0$, the plots do not extend much beyond $\tan\beta = 5$. This is caused by the constraint of unitarity in the Higgs–Higgs scattering sector [21]. At the higher values of $\tan\beta$, there is also a narrowing of the allowed region, largely due to the constraints following from $\Delta\rho$ and the B physics [20,21].

The surfaces representing $\langle\xi_1\rangle$ and $\langle\xi_2\rangle$ in Fig. 2 are in fact quite reminiscent of the corresponding averages of λ_1 and $\mathrm{Re}\lambda_{345}$, respectively. The details of these correspondences depend on which domains of the $\boldsymbol{\alpha}$ space (in this case, α_1) is populated. Typically, only scattered regions are allowed [20].

On the other hand, in Fig. 3 we have scanned over the full range of values of α_2 and α_3, compatible with all the constraints.

From these figures, we see that in much of the $\tan\beta - M_{H^\pm}$ parameter space, there is a considerable enhancement of the trilinear couplings as compared with the corresponding trilinear coupling in the SM. This is consistent with the special case studied in Fig. 1.

Incorporating CP violation in the 2HDM, we see a considerable change in the behavior of the couplings as we go from Fig. 2 to Fig. 3. This reflects the fact seen in Fig. 1 that the couplings have a strong dependence on the mixing angles, and, thus, on how CP violation is incorporated in the model.

Furthermore, there is a rapid variation of the Higgs coupling ratios around $\tan\beta = \mathcal{O}(2)$. As we shall see in the following, this is accompanied by a strong variation as one scans across the different values of $\boldsymbol{\alpha}$.

The trilinear coupling has a rather complicated behavior across the $\tan\beta$– $M_{H^\pm}$ plane, despite the smoothening that is implicit in the averaging over $\boldsymbol{\alpha}$. As is evident from Fig. 1 for ξ_1, the ratios ξ_1 and ξ_2 of trilinear couplings also vary considerably over the parameter space of $\boldsymbol{\alpha}$. One measure of this variation is the *variance*, defined as

$$\sigma_i = \sqrt{\langle(\xi_i - \langle\xi_i\rangle)^2\rangle}. \tag{3.23}$$

In Fig. 4 we display the variances σ_1 and σ_2 corresponding to the upper panels of Fig. 3. This quantity (in units of the SM trilinear coupling) is seen to be quite considerable, in particular, for ξ_2 and for moderate values of $\tan\beta$.

For approach (B), when we keep all three neutral Higgs boson masses fixed, the behavior is smoother, as seen in Fig. 5. For the parameters considered (note that $\mu = 0$), the values of $\tan\beta$ extend up to about 5. We note that the quantity $\langle\xi_1\rangle$ is rather similar to that shown in Figs. 2 and 3, increasing more or less monotonically with $\tan\beta$. The ratio $\langle\xi_2\rangle$ differs more, exhibiting a bulge of rather strong $H_1H_1H_2$ coupling for $\tan\beta = 2$–3 and $M_{H^\pm} = 450$–500 GeV.

B. Charged–charged–neutral Higgs couplings

Although in this paper we are mainly concerned with the trilinear couplings of the neutral Higgs bosons, here we briefly discuss the trilinear couplings of the charged Higgs boson of the 2HDM [25]. These are given by

$$\lambda_{i+-} = \sum_{m=1,2,3} R_{im} b_m. \tag{3.24}$$

We note that the index m [like the indices n and o in Eq. (3.3)] refers to the weak interaction eigenstates (η_1,

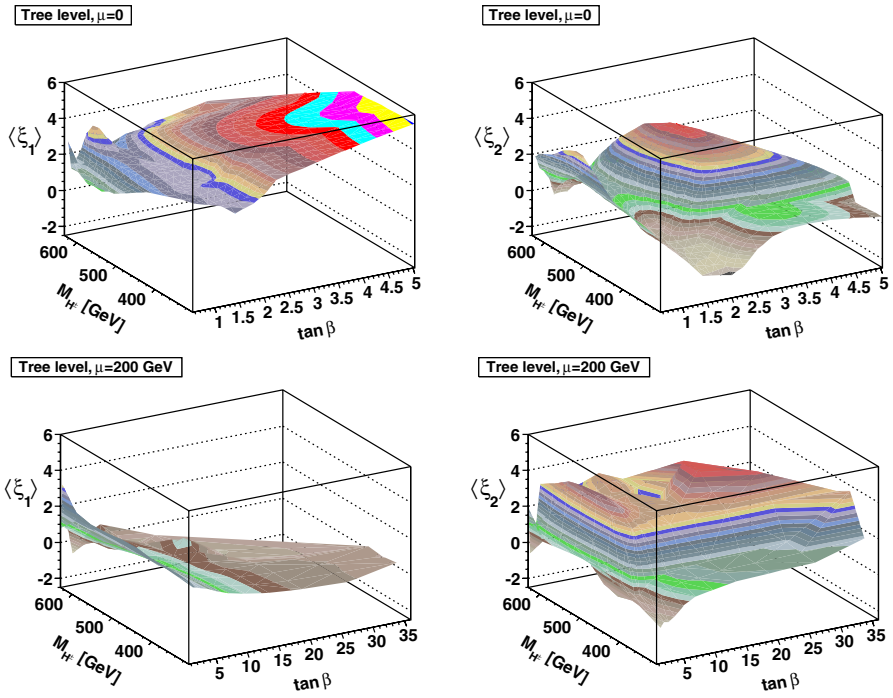

FIG. 3 (color online). Tree-level trilinear coupling ratios $\langle \xi_1 \rangle$ and $\langle \xi_2 \rangle$ as defined in Eq. (3.21), in approach (A), for the values of the Higgs masses $M_1 = 120$ GeV and $M_2 = 300$ GeV. For the top panel $\mu = 0$, whereas for the bottom panel $\mu = 200$ GeV. This plot is for the general case including CP violation, and is compatible with general constraints on the model.

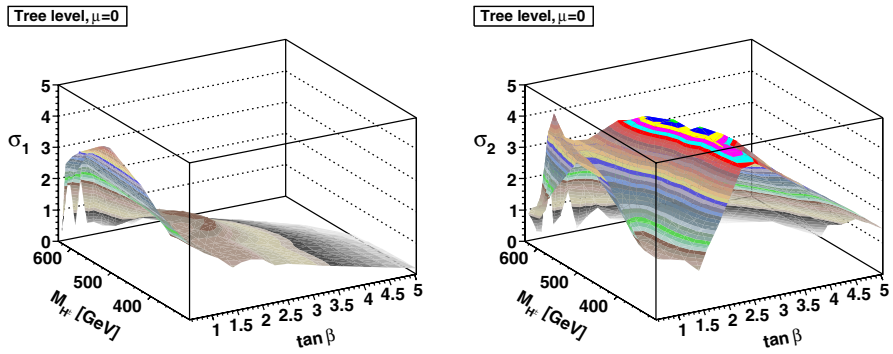

FIG. 4 (color online). Variance of trilinear coupling ratios ξ_1 and ξ_2 at the tree level. The parameters here correspond to the upper panels ($\mu = 0$) of Fig. 3.

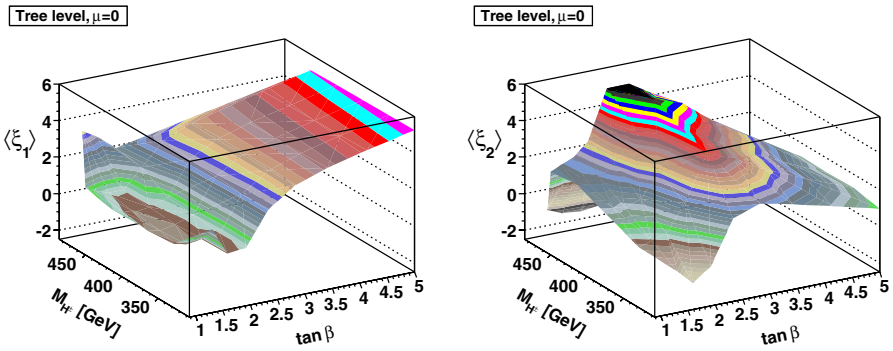

FIG. 5 (color online). Trilinear coupling ratios $\langle \xi_1 \rangle$ and $\langle \xi_2 \rangle$ at the tree level [see Eq. (3.21)], for approach (B), with $M_1 = 120$ GeV, $M_2 = 300$ GeV, $M_3 = 400$ GeV, and $\mu = 0$.

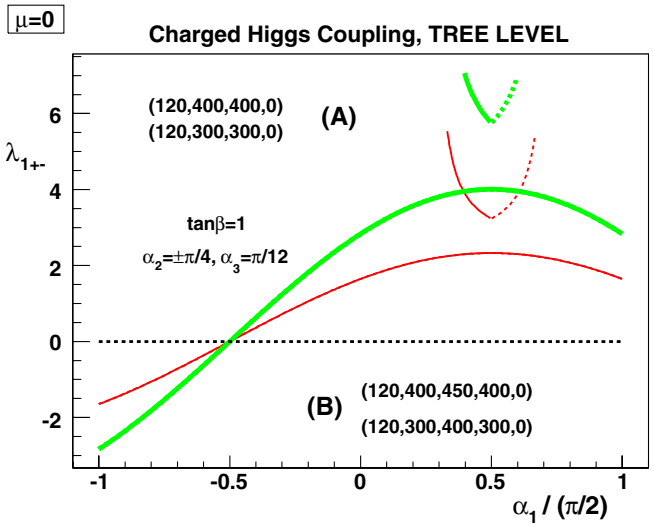

FIG. 6 (color online). The trilinear coupling λ_{1+-} at the tree level as a function of α_1, for two different values of α_2 ($-\pi/4$, dashed line, and $+\pi/4$, solid line), both with $\alpha_3 = \pi/12$. The masses and parameters are the same as in Fig. 1.

η_2 and η_3) of Eq. (2.4). The coefficients b_m in (3.24) can be written as (in units of $-iv$):

$$\begin{aligned} b_1 &= \cos\beta\{\sin^2\beta(\lambda_1 - \lambda_4 - \mathrm{Re}\lambda_5) + \cos^2\beta\lambda_3 \\ &\quad + \cos\beta\sin\beta[(\tan^2\beta - 2)\,\mathrm{Re}\lambda_6 + \mathrm{Re}\lambda_7]\}, \\ b_2 &= \sin\beta\{\cos^2\beta(\lambda_2 - \lambda_4 - \mathrm{Re}\lambda_5) + \sin^2\beta\lambda_3 \\ &\quad + \cos\beta\sin\beta[\mathrm{Re}\lambda_6 + (\cot^2\beta - 2)\,\mathrm{Re}\lambda_7]\}, \\ b_3 &= \cos\beta\sin\beta\,\mathrm{Im}\lambda_5 - \sin^2\beta\,\mathrm{Im}\lambda_6 - \cos^2\beta\,\mathrm{Im}\lambda_7. \end{aligned} \tag{3.25}$$

In Fig. 6 we display the coupling of H_1 to the charged H^+H^- pair, for the same choice of parameters as in Fig. 1. We note that in approach (B), with $\tan\beta = 1$ and $\mathrm{Im}\lambda_5 = 0$, this coupling has two interesting features: (1) It does not depend on the sign of α_2; and (2) it passes through zero for $\alpha_1 = -\pi/4$. The independence from the sign of α_2 can be understood in the following manner. For $i = 1$, the first two terms in Eq. (3.24) (proportional to R_{11} and R_{12}) contribute terms which are odd in α_2, arising from λ_1, λ_2, and λ_3. These odd parts are proportional to $(M_3^2 - M_2^2)$, and cancel against odd parts coming from the third term in (3.24), which are proportional to $\mathrm{Im}\lambda_6 + \mathrm{Im}\lambda_7$, which in turn is proportional to $\mathcal{M}_{13} + \mathcal{M}_{23}$.

Furthermore, the vanishing of the coupling at $\alpha_1 = -\pi/4$ can be understood as follows. In approach (B), with $\tan\beta = 1$ and $\alpha_1 = -\pi/4$, we have (see Eqs. (3.1) and (3.2) of Ref. [17])

$$\begin{aligned} \lambda_1(\alpha_2, \alpha_3) &= \frac{1}{v^2}[c_2^2 M_1^2 + (c_3 - s_2 s_3)^2 M_2^2 \\ &\quad + (s_3 + s_2 c_3)^2 M_3^2 - \mu^2], \\ \lambda_2(\alpha_2, \alpha_3) &= \frac{1}{v^2}[c_2^2 M_1^2 + (c_3 + s_2 s_3)^2 M_2^2 \\ &\quad + (s_3 - s_2 c_3)^2 M_3^2 - \mu^2]. \end{aligned} \tag{3.26}$$

Thus, for these particular values of $\tan\beta$ and α_1, $\lambda_2(-\alpha_2, \alpha_3) = \lambda_1(\alpha_2, \alpha_3)$, the first two terms in Eq. (3.24) cancel, and we are left with

$$\lambda_{1+-} = R_{13} b_3 = \tfrac{1}{2} s_2(\mathrm{Im}\lambda_5 - \mathrm{Im}\lambda_6 - \mathrm{Im}\lambda_7) = 0, \tag{3.27}$$

where in the last step we have used $\mathrm{Im}\lambda_5 = 0$, and the relations [see Eq. (2.19)]

$$\mathrm{Im}\,\lambda_5 + \mathrm{Im}\lambda_6 + \mathrm{Im}\lambda_7 = -\frac{\sqrt{2}}{v^2}[\mathcal{M}_{13}^2 + \mathcal{M}_{23}^2], \tag{3.28}$$

valid for $\tan\beta = 1$, and

$$\mathcal{M}_{13}^2 + \mathcal{M}_{23}^2 = 0, \tag{3.29}$$

valid for $\alpha_1 = -\pi/4$.

In Fig. 7, we show the coupling of the lightest neutral Higgs bosons to the charged Higgs bosons, averaged over $\boldsymbol{\alpha}$, in approach (A). Corresponding to what we observed in Fig. 6, these averages over $\boldsymbol{\alpha}$ also vanish along certain lines in the parameter space.

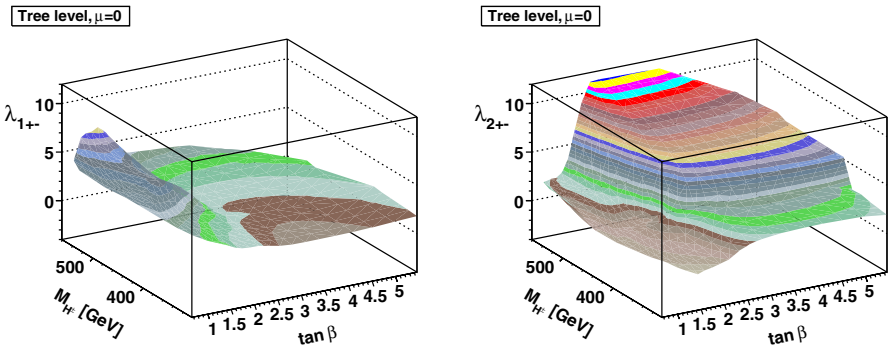

FIG. 7 (color online). Tree-level trilinear couplings λ_{1+-} and λ_{2+-} (in units of $-iv$) of the two lightest neutral Higgs bosons, H_1 and H_2, to a charged pair for $M_1 = 120$ GeV, $M_2 = 300$ GeV, and $\mu = 0$. The couplings are averaged over $\boldsymbol{\alpha}$, and have been plotted for approach (A).

IV. ONE-LOOP CORRECTIONS TO THE HIGGS BOSON MASSES

A. One-loop effective potential

For a realistic computation of the Higgs boson properties in the 2HDM, we must take into account the one-loop radiative corrections to the tree-level potential (2.2). When this is done, the relations among masses and the couplings of the tree-level potential undergo a change. In the MSSM, this effect, which is dominated by the top (and stop) quark contributions, is known to be very important [45] (see also Ref. [46]). In the 2HDM, there being no one-loop contribution from squarks, the main contributions at one loop are generated by the Higgs bosons. We shall here study the one-loop radiative corrections to the neutral Higgs sector using the method of one-loop effective potential [47]. The one-loop corrections to the tree-level potential (2.2) are given by

$$\Delta V = \frac{1}{64\pi^2}\Big[\sum_{\text{bosons}} M^4\Big(\log\frac{M^2}{Q^2} - \frac{3}{2}\Big) - \sum_{\text{fermions}} M^4\Big(\log\frac{M^2}{Q^2} - \frac{3}{2}\Big)\Big], \tag{4.1}$$

where the sums run over all bosonic and fermionic degrees of freedom, respectively, and Q^2 represents the scale at which the couplings are evaluated. As indicated above, the dominant contributions to (4.1) come from the Higgs bosons (neutral and charged), and the top quarks, all of which we will calculate in this section. Taking into account the spin, charge, and color degrees of freedom, we obtain

$$\begin{aligned}\Delta V &= \Delta V_{\text{neutral Higgs}} + \Delta V_{\text{charged Higgs}} + \Delta V_{\text{top}} \\ &= \frac{1}{64\pi^2}\sum_{\ell=1}^{3}\Big[M_\ell^4\Big(\log\frac{M_\ell^2}{Q^2} - \frac{3}{2}\Big)\Big] \\ &\quad + \frac{1}{32\pi^2} M_{H^\pm}^4\Big(\log\frac{M_{H^\pm}^2}{Q^2} - \frac{3}{2}\Big) \\ &\quad - \frac{3}{16\pi^2} m_t^4\Big(\log\frac{m_t^2}{Q^2} - \frac{3}{2}\Big),\end{aligned} \tag{4.2}$$

where all masses are understood to be field-dependent masses. Thus, after differentiation analogous to the one in Eq. (2.9) for the tree-level potential, for example, we do *not* set the fields η_1, η_2, and η_3 to zero, but instead evaluate

$$\mathcal{M}^2_{ij}(\eta_1, \eta_2, \eta_3) = \frac{\partial}{\partial\eta_i}\frac{\partial}{\partial\eta_j} V(\eta_1, \eta_2, \eta_3, H^\pm, G^\pm), \tag{4.3}$$

and similarly

$$M^2_{H^\pm}(\eta_1, \eta_2, \eta_3) = \frac{\partial}{\partial H^+}\frac{\partial}{\partial H^-} V(\eta_1, \eta_2, \eta_3, H^\pm, G^\pm), \tag{4.4}$$

and after having performed the differentiation, we set $H^\pm = G^\pm = 0$.

At tree level, the three minimization conditions (2.18) (two real, and one imaginary) can be used to eliminate the bilinear parameters m_1^2 and m_2^2, as well as relate $\mathrm{Im}\lambda_5$ to $\mathrm{Im}\, m_{12}^2$. At the one-loop level, the expressions for m_1^2 and m_2^2 are modified due to the contributions coming from $\partial\Delta V/\partial\eta_1$ and $\partial\Delta V/\partial\eta_2$. This amounts to adjusting the parameters of the potential such that the minimum is stationary in terms of the same vacuum expectation values v_1 and v_2 as for the tree-level potential (i.e., $\tan\beta$ remains unchanged). In the following we shall calculate the different contributions to the neutral Higgs boson masses arising from (4.2) using the above procedure.

B. One-loop corrections to Higgs masses

The mass squared matrix for the neutral Higgs bosons will receive contributions from one-loop effects due to neutral Higgs bosons, which can be written as

$$\frac{\partial^2\Delta V_{\text{neutral Higgs}}}{\partial\eta_i\partial\eta_j} = \frac{1}{32\pi^2}\sum_{\ell=1}^{3}\Big[\log\frac{M_\ell^2}{Q^2}\frac{\partial M_\ell^2}{\partial\eta_i}\frac{\partial M_\ell^2}{\partial\eta_j} + M_\ell^2\Big(\log\frac{M_\ell^2}{Q^2} - 1\Big)\frac{\partial^2 M_\ell^2}{\partial\eta_i\partial\eta_j}\Big]. \tag{4.5}$$

The derivatives of M_ℓ^2 with respect to the fields η_i, which are rather involved, are discussed in detail in Appendix C.

The corresponding second derivatives of the charged-Higgs-field-dependent part of the one-loop corrections to the potential, $\Delta V_{\text{charged Higgs}}$, in (4.2) are given by

$$\frac{\partial^2\Delta V_{\text{charged Higgs}}}{\partial\eta_i\partial\eta_j} = \frac{1}{16\pi^2}\Big[\log\frac{M_{H^\pm}^2}{Q^2}\frac{\partial M_{H^\pm}^2}{\partial\eta_i}\frac{\partial M_{H^\pm}^2}{\partial\eta_j} + M_{H^\pm}^2\Big(\log\frac{M_{H^\pm}^2}{Q^2} - 1\Big)\frac{\partial^2 M_{H^\pm}^2}{\partial\eta_i\partial\eta_j}\Big]. \tag{4.6}$$

Finally, there are one-loop corrections due to the top quark, which can be written as

$$\frac{\partial^2\Delta V_{\text{top}}}{\partial\eta_i\partial\eta_j} = -\frac{3}{2\pi^2}\frac{m_t^4}{v_2^2}\Big(2\log\frac{m_t^2}{Q^2} - 1\Big)\delta_{i2}\delta_{j2}, \tag{4.7}$$

where in the last equation we have used $\partial m_t/\partial\eta_i = (m_t/v_2)\delta_{i2}$. We neglect the contributions from lighter fermions.

The full one-loop mass-squared matrix for the neutral Higgs bosons can, thus, be written as a sum of four terms:

$$\mathcal{M}^2_{ij}(\eta_1, \eta_2, \eta_3) = \mathcal{M}^2_{\text{tree},ij}(\eta_1, \eta_2, \eta_3) + \frac{\partial^2\Delta V_{\text{neutral Higgs}}}{\partial\eta_i\partial\eta_j} + \frac{\partial^2\Delta V_{\text{charged Higgs}}}{\partial\eta_i\partial\eta_j} + \frac{\partial^2\Delta V_{\text{top}}}{\partial\eta_i\partial\eta_j}. \tag{4.8}$$

From the mass-squared matrix (4.8), the eigenvalues

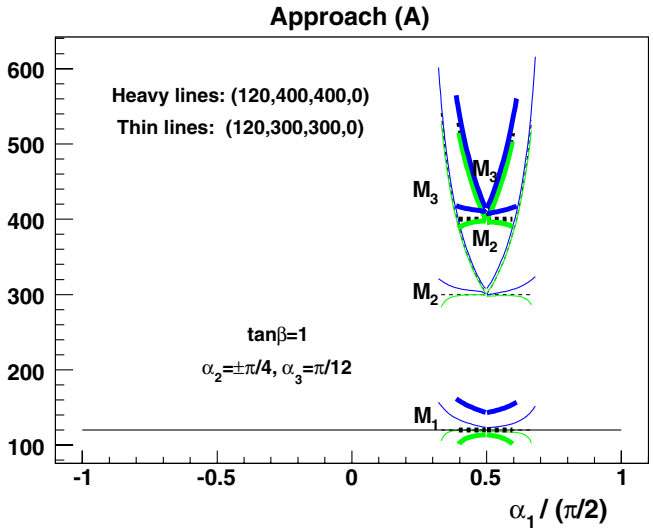

FIG. 8 (color online). One-loop Higgs masses M_1, M_2 and M_3 (in units of GeV) plotted as functions of α_1, with $\alpha_2 = \pm\pi/4$, both with $\alpha_3 = \pi/12$. The lowest-order Higgs masses are $M_1^{\rm LO} = 120$ GeV, with $M_2^{\rm LO} = M_{H^\pm}^{\rm LO} = 300$ GeV (thin lines), and $M_2^{\rm LO} = M_{H^\pm}^{\rm LO} = 400$ GeV (heavy lines). Here $\mu = 0$ and $\tan\beta = 1$. Dashed lines refer to tree-level values, whereas green and blue lines refer to one-loop corrected results, with the scale parameter $Q = 2M_1^{\rm LO}$ and $Q = 500$ GeV, respectively.

$M_\ell(\eta_1, \eta_2, \eta_3)$ can be determined. These are the one-loop corrected masses for the neutral Higgs bosons.

In Fig. 8 we show, for approach (A), the one-loop corrected Higgs boson masses, corresponding to the trilinear couplings studied in Fig. 1 (i.e., with α_2 and α_3 held fixed), due to the one-loop radiative corrections discussed above. The superscript "LO" here denotes lowest-order values. The Higgs boson masses are determined as eigenvalues of the matrix (4.8), evaluated for $\eta_1 = \eta_2 = \eta_3 = 0$. The full η-dependence, to be discussed in the next section, will however be required for evaluating the one-loop trilinear Higgs couplings.

The following points are worth noting here: (i) The tree-level value of M_3, namely $M_3^{\rm LO}$, has a strong dependence on α_1. This is a consequence of keeping $M_1^{\rm LO}$, $M_2^{\rm LO}$, α_2, and α_3 fixed. (ii) The one-loop corrections have a significant dependence on the scale at which they are evaluated, as is illustrated by comparing the values of the Higgs boson masses at two different values of Q^2. (iii) The one-loop correction to the Higgs boson mass can be either positive or negative. (iv) At some of the boundaries of the allowed parameter space, these one-loop corrections become large.

The reason for the strong variation of M_3 at the edges of the allowed parameter space can be found from an inspection of the different origin of such edges. These can be described as follows:

(1) In approach (A), at tree level, $(M_3^{\rm LO})^2$ is determined as a rational fraction, where the numerator is linear in $(M_1^{\rm LO})^2$ and $(M_2^{\rm LO})^2$ (multiplying rotation matrix elements and $\tan\beta$), whereas the denominator is a linear function in rotation matrix elements and $\tan\beta$. (For an explicit formula, see Eq. (4.16) of Ref. [19].) For critical values of the rotation matrix elements, e.g., when $R_{31} = R_{32}\tan\beta$, the denominator will pass through zero. At such points, $M_3^{\rm LO}$ diverges, and the allowed parameter space terminates.
(2) In approach (A), M_3^2 may at some critical values of the rotation matrix elements become equal to M_2^2. This happens when either $R_{13} = 0$ or $R_{12}\tan\beta = R_{11}$ [19]. In the former case we have $\alpha_2 = 0$ (α_1 and α_3 being arbitrary), whereas in the latter we have $\tan\beta = \cot\alpha_1$ (α_2 and α_3 being arbitrary).
(3) Positivity may break down.
(4) Perturbative unitarity may break down.
(5) Parameter space may be truncated by some experimental constraint.

The first two of these cases are illustrated in Fig. 8. We actually exclude, as "unphysical," regions where $M_1 < 100$ GeV (for $M_1^{\rm LO} = 120$ GeV) and where either $M_3^{\rm LO} > 2M_2^{\rm LO}$ or $M_3 > 2M_2$.

For approach (A), positivity is expressed in terms of simple inequalities, whereas for approach (B), with α_6 and α_7 nonzero, an involved numerical test is required [20]. Perturbative unitarity in the Higgs–Higgs scattering sector tends to truncate high values of $\tan\beta$, unless μ is large (comparable to M_2) [17].

Having described the radiative corrections to the Higgs masses, we next show in Fig. 9 typical one-loop multiplicative mass corrections, i.e., $M_1/M_1^{\rm LO}$ and $M_2/M_2^{\rm LO}$ for the case $M_1^{\rm LO} = 120$ GeV, $M_2^{\rm LO} = 300$ GeV, and $\mu = 0$. (This will be discussed in more detail in Sec. VII.) The renormalization scale has been chosen as $Q^2 = (2M_1^{\rm LO})^2$. As in Sec. III, an average over allowed points in $\boldsymbol{\alpha}$ has been performed.

For M_1, the loop correction is [for $Q^2 = (2M_1^{\rm LO})^2$] negative at low values of $\tan\beta$, whereas it is positive for higher values. For M_2, on the other hand, the correction is smaller, and has no strong dependence on $\tan\beta$. The negative correction for M_1 is different from the MSSM, where the one-loop corrections, dominated by the top-quark (squark) contribution, is positive. Here, it is the Higgs sector which dominates, and this contribution has the opposite sign, because of the bosonic nature of the contributing particles in the loop. In actual practice the situation is more complicated, since different Higgs fields may contribute with different signs, depending on how the mass of the respective Higgs boson compares with the scale Q.

In view of the fact that the one-loop correction to M_1 can be significant, and negative, we impose the constraint of LEP2 nondiscovery of a Higgs boson on the one-loop corrected lightest Higgs boson mass. Higgs boson masses below the "magic" 114.4 GeV value are of course allowed, provided the coupling to the Z and $b\bar{b}$ (or τ pairs) are suppressed.

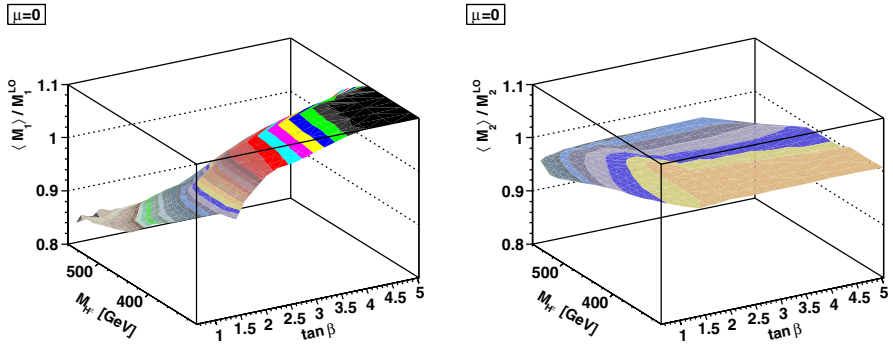

FIG. 9 (color online). One-loop multiplicative mass correction for tree-level mass parameters $M_1 = 120$ GeV, $M_2 = 300$ GeV, and $\mu = 0$.

Treating the loop corrections as a perturbation, we have here imposed the theoretical and experimental constraints on the tree-level parameters. We note that at low values of $\tan\beta$, the mass of the lightest Higgs boson, M_1, may be considerably reduced. When we proceed to study the trilinear couplings, we shall therefore impose the LEP2 non-discovery constraint on the loop-corrected mass, M_1. For a higher scale parameter, though, the mass may increase also at low values of $\tan\beta$.

V. ONE-LOOP CORRECTIONS TO THE TRILINEAR HIGGS COUPLINGS

The one-loop corrected trilinear Higgs couplings are given by the third-order derivatives of the one-loop effective potential with respect to different fields. We shall separately consider the contributions to the potential from the neutral Higgs fields, the charged Higgs fields and the top-quark fields. We start the calculation by evaluating the derivatives with respect to the weak fields, which can then be converted to derivatives with respect to the fields corresponding to the mass eigenstates with the help of Eq. (3.2).

The starting point of the calculation of the one-loop corrections to the trilinear Higgs couplings is the expression (4.2). From this we obtain the one-loop radiative corrections to the trilinear Higgs couplings due to neutral Higgs bosons as

$$\frac{\partial^3 \Delta V_{\text{neutral Higgs}}}{\partial\eta_i\partial\eta_j\partial\eta_k} = \frac{1}{32\pi^2}\sum_{\ell=1}^{3}\Bigg[\frac{1}{M_\ell^2}\frac{\partial M_\ell^2}{\partial\eta_i}\frac{\partial M_\ell^2}{\partial\eta_j}\frac{\partial M_\ell^2}{\partial\eta_k} + \log\frac{M_\ell^2}{Q^2}\Bigg(\frac{\partial^2 M_\ell^2}{\partial\eta_i\partial\eta_j}\frac{\partial M_\ell^2}{\partial\eta_k} + \frac{\partial^2 M_\ell^2}{\partial\eta_j\partial\eta_k}\frac{\partial M_\ell^2}{\partial\eta_i} + \frac{\partial^2 M_\ell^2}{\partial\eta_k\partial\eta_i}\frac{\partial M_\ell^2}{\partial\eta_j}\Bigg) + M_\ell^2\Bigg(\log\frac{M_\ell^2}{Q^2} - 1\Bigg)\times\frac{\partial^3 M_\ell^2}{\partial\eta_i\partial\eta_j\partial\eta_k}\Bigg]. \tag{5.1}$$

The derivatives of squared masses with respect to the weak fields η_i in (5.1) are evaluated and discussed in Appendix C.

To find one-loop charged Higgs boson correction to the trilinear couplings, we start with *field-dependent* squared masses, $M^2_{H^\pm}(\eta_1, \eta_2, \eta_3)$, for the charged Higgs boson. Noting that the potential is a function of masses, i.e., $\Delta V_{\text{charged Higgs}} = \Delta V(\eta_1, \eta_2, \eta_3)$, we obtain

$$\frac{\partial^3 \Delta V_{\text{charged Higgs}}}{\partial\eta_i\partial\eta_j\partial\eta_k} = \frac{1}{16\pi^2}\Bigg[\frac{1}{M^2_{H^\pm}}\frac{\partial M^2_{H^\pm}}{\partial\eta_i}\frac{\partial M^2_{H^\pm}}{\partial\eta_j}\frac{\partial M^2_{H^\pm}}{\partial\eta_k} + \log\frac{M^2_{H^\pm}}{Q^2}\Bigg(\frac{\partial^2 M^2_{H^\pm}}{\partial\eta_i\partial\eta_j}\frac{\partial M^2_{H^\pm}}{\partial\eta_k} + \frac{\partial^2 M^2_{H^\pm}}{\partial\eta_j\partial\eta_k}\frac{\partial M^2_{H^\pm}}{\partial\eta_i} + \frac{\partial^2 M^2_{H^\pm}}{\partial\eta_k\partial\eta_i}\frac{\partial M^2_{H^\pm}}{\partial\eta_j}\Bigg)\Bigg]. \tag{5.2}$$

For the one-loop corrections arising from the top-quark, we note that in Model II (which we consider) the up-type quarks couple only to Φ_2 (and not to Φ_1). Thus, the one-loop contribution due to top quark affects only the fields η_2. We can then write

$$\frac{\partial^3 \Delta V_{\text{top}}}{\partial\eta_i\partial\eta_j\partial\eta_k} = -\frac{12}{\pi^2}\frac{m_t^4}{v_2^3}\log\frac{m_t^2}{Q^2}\delta_{i2}\delta_{j2}\delta_{k2}. \tag{5.3}$$

VI. QUANTITATIVE RESULTS FOR TRILINEAR HIGGS COUPLINGS

We have seen that the lowest order trilinear couplings are highly dependent on the details of the two Higgs doublet model. This sensitivity on the details of the model is actually enhanced when we take into account the one-loop corrections to the Higgs potential. The loop corrections to the trilinear couplings can vary strongly with the parameters of the model, and also have a considerable dependence on the scale Q^2 used in Eqs. (5.1), (5.2), and (5.3).

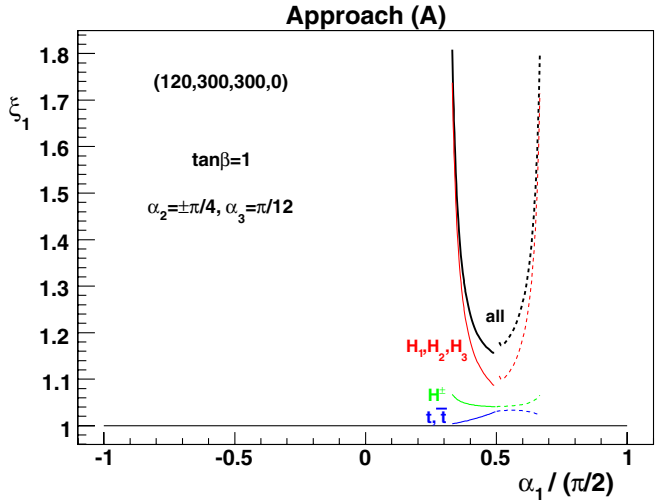

FIG. 10 (color online). Contributions to the trilinear coupling ratio ξ_1 plotted as functions of α_1, for $\alpha_2 = \pm\pi/4$, both with $\alpha_3 = \pi/12$. The Higgs mass and parameters are as in Fig. 1. The scale parameter is $Q = 2M_1^{\rm LO}$. The full correction is shown by the upper, heavy black lines, whereas partial contributions from neutral and charged Higgs bosons, as well as from top quarks, are shown by the thin red, green, and blue lines.

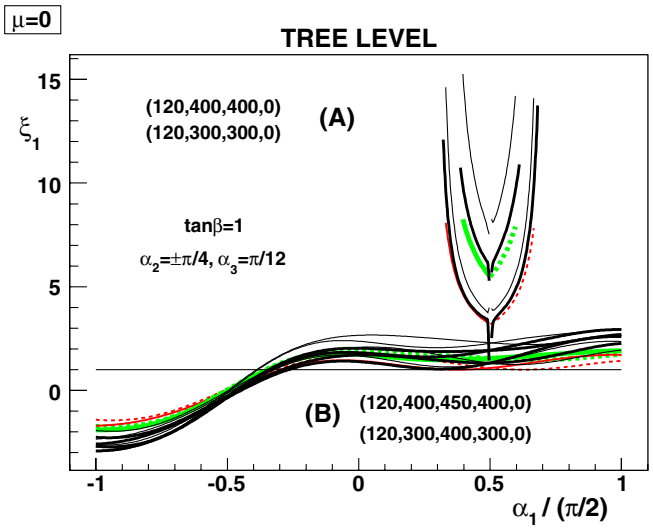

FIG. 11 (color online). Trilinear coupling ratio ξ_1 [see Eq. (3.8)] as a function of α_1. Colored lines refer to tree-level results (same color coding and parameters as in Fig. 1), black lines refer to loop-corrected results (thin: $Q = 2M_1^{\rm LO}$, heavy: $Q = 500$ GeV).

A. Different contributions

For fixed values of α_2 and α_3, as in Fig. 1, we show in Fig. 10 the ratio of the one-loop corrected trilinear Higgs coupling λ_{111} and the corresponding tree-level coupling. This ratio is highly dependent on α_1 (as is the coupling itself).

As compared with the one-loop corrections to the masses, the corrections to the trilinear couplings are relatively much larger. The following two points are worth noting: (i) Most of the one-loop contribution comes from the neutral-Higgs term, Eq. (5.1) (red lines labeled "H_1, H_2, H_3"). (ii) The correction can be very large at the boundary of the physically allowed region (in this case, in α_1). These regions of very large corrections, which are excluded from averages over $\boldsymbol{\alpha}$, will be discussed further in the following.

In approach (A), when we scan over the values of $\boldsymbol{\alpha}$, there are regions where M_3 gets very close to M_2. From Ref. [19], we see that (at tree level) this happens when (i) $\alpha_2 \to 0$ or (ii) $\tan\beta \to \cot\alpha_1$, or (iii) $\alpha_2 \to \pm\pi/2$. Case (ii) occurs for $\tan\beta = 1$ and $\alpha_1 = \pi/4$. In this region, the trilinear coupling tends to get very large. This is clearly a region of parameter space where the present approach breaks down. In the notation of Appendix C [see Eq. (C12)], we see that two roots merge ($M_3 \to M_2$) when the complex phases of s_1 and s_2 differ by $2\pi/3$. Near such points, the derivatives of s_1 and s_2 with respect to a and b, particularly the second and third-order ones, tend to get very large. Actually, such points have been removed from the following figures, and we impose a cut when scanning over $\boldsymbol{\alpha}$ in Sec. VI D:

$$\min\{(M_3^{\rm LO} - M_2^{\rm LO}), (M_3 - M_2)\} > 5 \text{ GeV}. \qquad (6.1)$$

B. Scale dependence

Just as in the case of one-loop corrections to the masses, we note a strong dependence of the trilinear couplings on the scale parameter that enters the effective potential. This scale plays a role somewhat analogous to the mass scale of superpartners in the effective-potential approach to the MSSM.

In Fig. 11 we study the one-loop corrected trilinear couplings, for both the approaches (A) and (B), and for two sets of Higgs masses within each approach (the same as in Fig. 1). We show how the one-loop corrections depend on the scale Q. For this purpose we have considered two timelike values of Q, namely, $Q = 2M_1^{\rm LO}$ and $Q = 500$ GeV. As in the case of Fig. 10, we see that in approach (A), the couplings tend to get large near the boundary of the allowed parameter space. (Near $\alpha_1 = \pi/4$, we notice the irregular behavior discussed in Sec. VI A, when $M_3 \to M_2$.)

The dependence on the scale is rather involved, but there is a tendency that a lower scale gives a larger correction. This is rather clear in the upper part of the figure, which is a plot for approach (A). For approach (B), however, we have not labeled the individual curves, the main point being to show that there is a considerable uncertainty related to the choice of scale in both approaches.

C. Decoupling

In the context of the trilinear Higgs coupling, decoupling would imply that the self-coupling of the light Higgs boson

could be expressed in terms of its mass, as in the standard model. This was indeed found to hold for the MSSM, if the mass is taken to be the loop-corrected one [28,29].

In order to discuss decoupling in the 2HDM, we first need to define, as a reference, a standard-model-like limit by imposing the tree-level constraint (3.11), together with Eq. (3.22). The SM-like nature of this limit may be extended to the loop level, if in the loop corrections (4.2) we include only the contributions of the lightest neutral Higgs boson H_1 and the top quark. Within this framework, we may then study decoupling, by defining the ratio, analogous to (3.21):

$$\langle \bar{\xi}_1 \rangle = \frac{\langle \lambda_{111}^{\rm full} \rangle}{\langle \lambda_{111}^{\rm SM} \rangle}, \tag{6.2}$$

where

(i) $\lambda_{111}^{\rm SM}$ includes only loop corrections due to $t\bar{t}$ and H_1, as would be the case in the SM.

(ii) $\lambda_{111}^{\rm full}$ includes all one-loop corrections to the Higgs coupling in the two Higgs doublet model, i.e., also those due to H_2, H_3, and $H^{\pm}$.

(iii) The averaging over α_2 and α_3 is constrained by Eq. (3.22) with $\alpha_0 = 0.025 \times \pi/2$, whereas α_1 is left unconstrained.

It should be noted that here we do not insist on a correspondence between the 2HDM and the MSSM, since this would require also $\alpha_1 \simeq \beta$.

If the ratio (6.2) were to come out as unity, it would be a signal for decoupling: the heavy Higgs bosons do not affect the coupling of the lightest one with itself. In Fig. 12, we display this ratio, for rather high values of $M_2^{\rm LO}$ and μ: $M_2^{\rm LO} = \mu = 500$ GeV, subjecting all parameters to the general constraints discussed in Sec. III A. For $M_{H^{\pm}} \sim M_2$, the ratio (6.2) is indeed rather close to unity, *but for larger values of* $M_{H^{\pm}}$, *it becomes significantly larger*. In the region where $\langle \bar{\xi}_1 \rangle \lesssim 1.20$, we have also checked that $M_3 - M_2 < \mathcal{O}(40)$ GeV. Thus, in this region of the parameter space, decoupling holds at the loop level to about 10%–20%. For larger values of $M_{H^{\pm}}$, however, where the model is still consistent, decoupling is strongly violated.

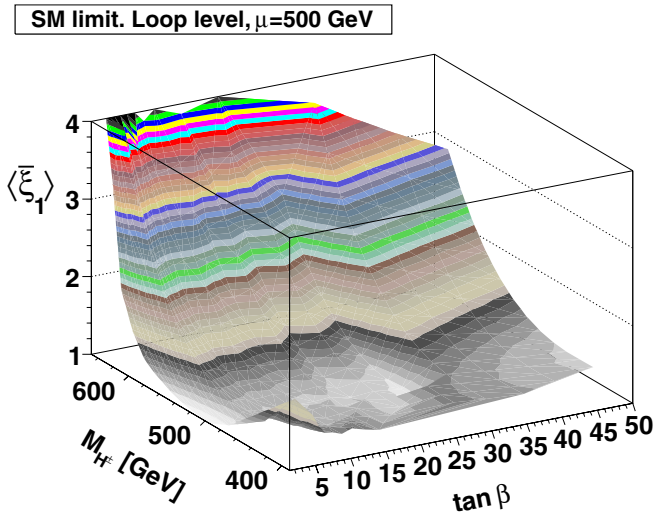

FIG. 12 (color online). Trilinear coupling ratio $\langle \bar{\xi}_1 \rangle$ as defined by Eq. (6.2). Different quantities in approach (A) with $M_1^{\rm LO} = 120$ GeV, $M_2^{\rm LO} = \mu = 500$ GeV, and $Q = 2M_1^{\rm LO}$. The ratio $\langle \bar{\xi}_1 \rangle \simeq 1$ demonstrates approximate decoupling for $M_2 = \mu \sim M_{H^{\pm}}$.

The result displayed in Fig. 12 is quite stable under a change of α_0 from $0.025 \times \pi/2$ to $0.05 \times \pi/2$. However, the result depends on the choice of scale adopted for evaluating the one-loop potential. For example, for $Q = 500$ GeV, $\langle \bar{\xi}_1 \rangle$ differs significantly from unity. This is perhaps contrary to expectations, since $\log(M_2^{\rm LO}/Q)$ then vanishes. However, we recall that (i) the one-loop potential also contains nonlogarithmic terms, and (ii) the one-loop potential modifies the minimization conditions, i.e., its contribution shifts the values of the soft parameters m_{11}^2 and m_{22}^2 of the tree-level potential.

In the 2HDM, in contrast to the MSSM, the decoupling cannot be exact. The reason is obvious: the heavy fields that we would like to neglect, are all bosonic, and thus all contribute with the same sign to the potential. Furthermore, even if we choose the scale Q such that the logarithms vanish, there would still be the nonlogarithmic remainders.

The question of decoupling can be illustrated by the behavior of the ρ parameter, which gets contributions from all *pairs* of Higgs bosons. These contributions vanish for equal masses, but are large when the masses are very different.

In the limit of no CP violation, custodial symmetry [48] would imply $M_{H^{\pm}} = M_j$, where M_j is either the mass of the CP odd (A) or a CP even (H) Higgs particle [49]. In the case that $M_{H^{\pm}} = A$, orthogonality of the even-sector mixing matrix would protect the $\Delta\rho$ parameter from large corrections. In the present case of CP violation, a higher degeneracy is required, $M_2 = M_3 = M_{H^{\pm}}$, in order to avoid large contributions to $\Delta\rho$. Since this is in general not satisfied, the experimental constraints on $\Delta\rho$ severely constrain the allowed parameter space [21], and there is no decoupling.

D. The general case

After this exploratory discussion, we are now ready to scan and average over the full range of $\boldsymbol{\alpha}$, compatible with theoretical and experimental constraints on the model, as was done at tree level in Sec. III A. Figures 13 and 14 are plotted for approach (A) with $M_1^{\rm LO} = 120$ GeV, $M_2^{\rm LO} = 300$ GeV, $\mu = 0$ (Fig. 13), $\mu = 200$ GeV (Fig. 14) and with scale $Q = 2M_1^{\rm LO}$ in both cases.

In these figures, we show the ratios $\langle \xi_1 \rangle$ and $\langle \xi_2 \rangle$ of trilinear couplings in the top panels. The middle panels are devoted to the loop-induced corrections to the masses M_1 and M_2, whereas the bottom panels show the variance associated with the averaging of ξ_1 and ξ_2 over the $\boldsymbol{\alpha}$ parameter space.

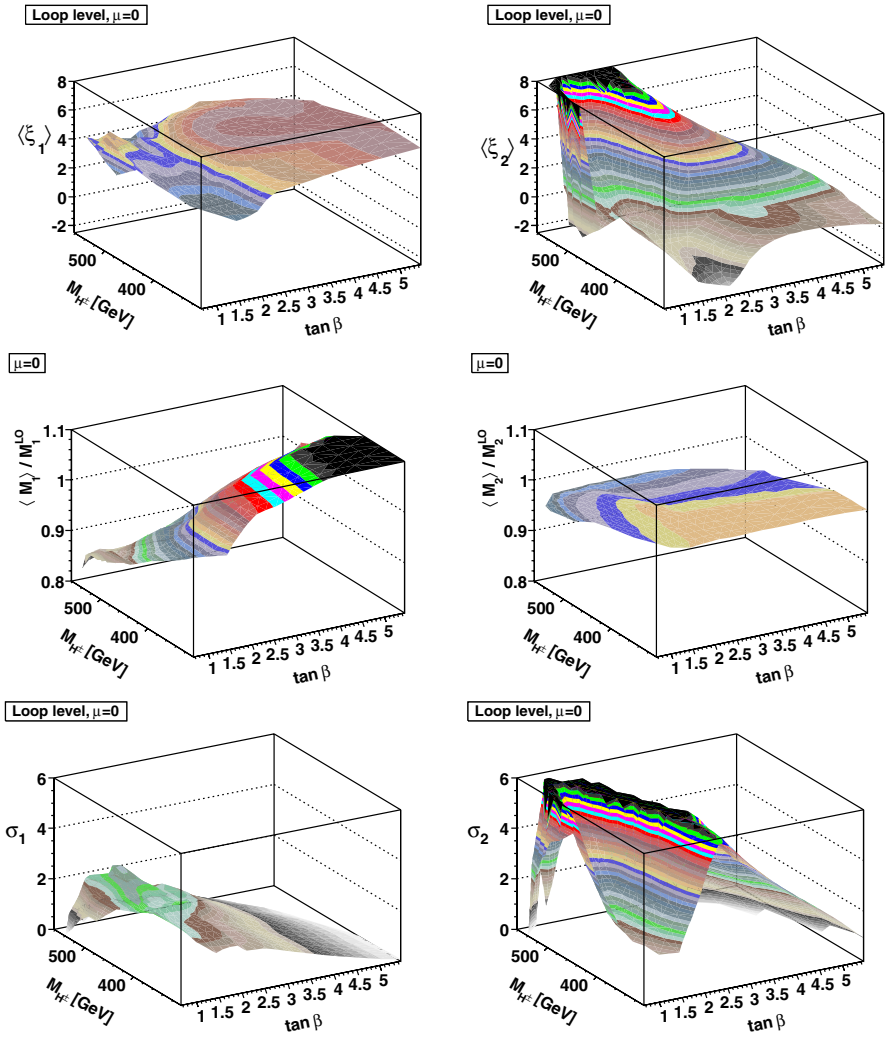

FIG. 13 (color online). Approach (A) with $M_1^{\rm LO} = 120$ GeV, $M_2^{\rm LO} = 300$ GeV, $\mu = 0$, and scale $Q = 2M_1^{\rm LO}$. Top panel: Trilinear coupling ratios $\langle \xi_1 \rangle$ and $\langle \xi_2 \rangle$ [see Eq. (3.21)]. Middle: one-loop multiplicative mass correction. Bottom: Variance of trilinear coupling ratios ξ_1 and ξ_2.

An important difference between the two cases presented in these figures is the range in $\tan\beta$. As already discussed, for a low value of μ, the high values of $\tan\beta$ would lead to a model that would violate unitarity, and are, therefore, excluded [20].

Comparing the top panels of Figs. 13 and 14 with the corresponding tree-level results shown in Fig. 3, we note the following: (i) The overall shape in the $\tan\beta$– $M_{H^\pm}$ plane is similar. (ii) The loop-corrected couplings are somewhat larger, after averaging over $\boldsymbol{\alpha}$, in analogy with the results shown in Fig. 11 for α_2 and α_3 fixed.

The center panel of Fig. 13 is rather similar to Fig. 9, the only difference being that here the LEP2 constraint is imposed at the loop level. Focusing first on the loop corrections to M_1, and comparing the mass correction at the two different values of μ, we note that the case $\mu = 0$ gives a larger reduction at low values of $\tan\beta$ and a larger increase at high values of $\tan\beta$. For M_2, on the other hand, the loop correction has only a rather weak dependence on $\tan\beta$ (and $M_{H^\pm}$). For a higher value of the scale Q, however, the loop correction to M_1 may be positive also at low values of $\tan\beta$.

The trilinear couplings represented in these figures, are of course not physical, they are instead "typical values," obtained by an averaging over the angles of the mixing matrix R that diagonalizes the mass-squared matrix. As discussed above, the variation over the $\boldsymbol{\alpha}$ parameter space can be considerable, as illustrated by the *variance* shown in the bottom panels.

A more detailed comparison reveals that the loop corrections are most important for low values of $\tan\beta$. This is particularly so in the case of $\langle \xi_2 \rangle$, where the variance is also quite large. This is in part caused by the ill-defined limit $M_3 \to M_2$ ($\alpha_2 \to 0$) discussed above. [Actually, at high values of $M_{H^\pm}$, the $\langle \xi_2 \rangle$ plots are truncated at the top.]

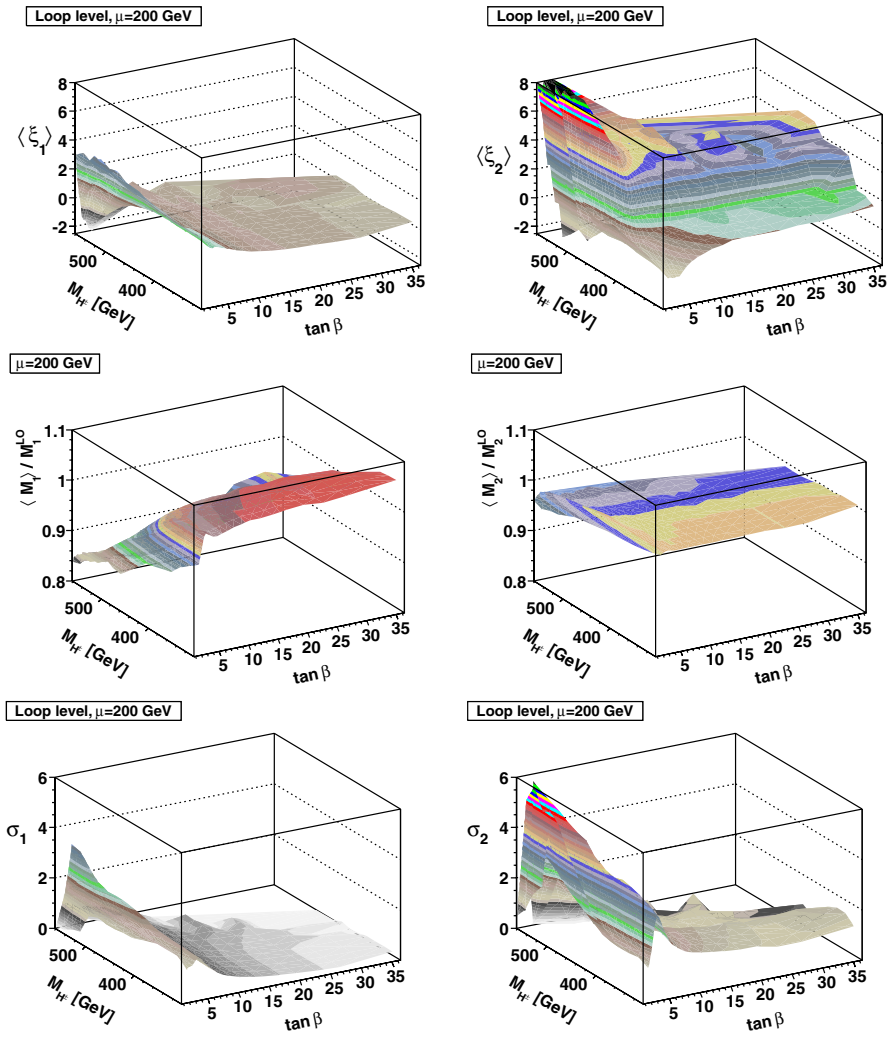

FIG. 14 (color online). Same as Fig. 13, but with $\mu = 200$ GeV.

The correlation between these trilinear couplings and the quartic couplings λ_i of the tree-level potential or their averages, $\langle\lambda_i\rangle$, is not very simple, but a couple of observations can be made. In Fig. 13, for $\mu = 0$ the enhancement at low values of $\tan\beta$ is correlated with a corresponding enhancement of $\langle\lambda_2\rangle$, whereas $\langle\lambda_1\rangle$ is large at high values of $\tan\beta$.

For the $H_1H_1H_1$ coupling, represented by $\langle\xi_1\rangle$, we note that for $\mu = 0$ it is rather large for all values of $\tan\beta$ and $M_{H^\pm}$ where the model is consistent, whereas for $\mu = 200$ GeV it falls to zero for large values of $\tan\beta$.

Finally, in Fig. 15 we show the behavior for somewhat higher value of the soft mass parameter, $\mu = 500$ GeV. We display the averages $\langle\xi_1\rangle$ and $\langle\xi_2\rangle$ for two values of $M_2^{\rm LO}$, 300 GeV (as was adopted in the earlier plots) and 500 GeV. Compared to the corresponding panels of Figs. 13 and 14, the present ones (for $\mu = 500$ GeV) are more smooth, and also somewhat different in magnitude.

VII. SUMMARY AND CONCLUSIONS

The two Higgs doublet model is a viable extension of the standard model Higgs sector. Apart from having a richer structure of Higgs bosons and Higgs couplings, it can accommodate *CP* violation beyond that of the Kobayashi–Maskawa mechanism in the SM. In this paper we have studied in detail the trilinear couplings of the lightest Higgs boson of this model, including the *CP* violating effects. Our main objective has been to study the implications of *CP* violation for the trilinear couplings of the general two Higgs doublet model. We have discussed two different parametrizations of the general two Higgs doublet model, and imposed the constraints on the parameters of the model following from theoretical considerations and from different experiments. Tree-level unitarity, B physics and $\Delta\rho$ are the most constraining ones for the parameters of the two Higgs doublet model with *CP* violation.

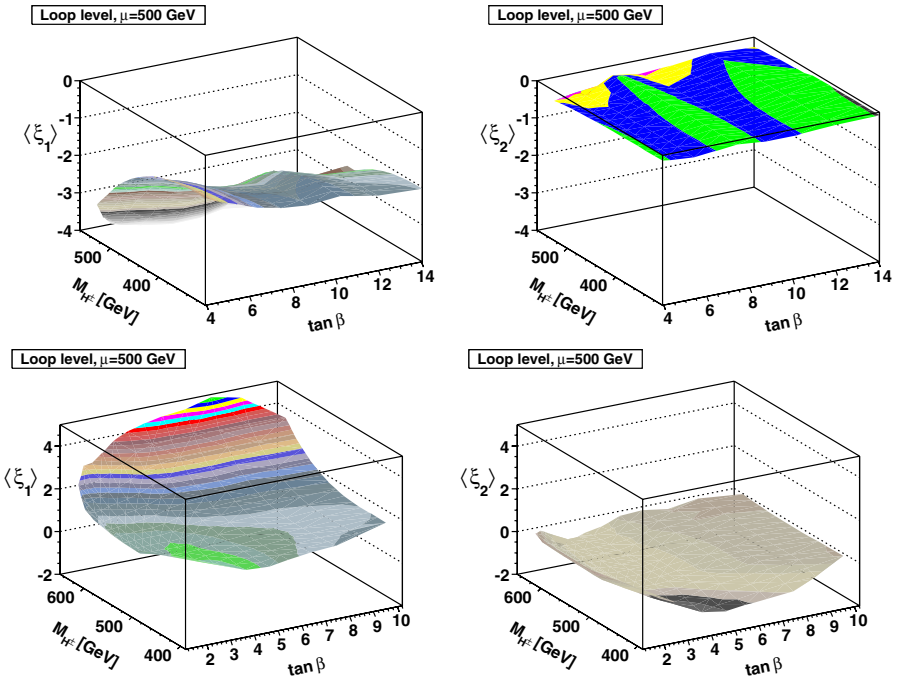

FIG. 15 (color online). Similar to the upper panels of Figs. 13 and 14, but for $\mu = 500$ GeV. Upper panels: $M_2^{\mathrm{LO}} = 300$ GeV; lower panels: $M_2^{\mathrm{LO}} = 500$ GeV. Note that the scales are different from those in the earlier figures.

Within the allowed domain of the parameter space of the model, the trilinear couplings can have a very strong dependence on the neutral Higgs boson mixing angles. Because of this strong dependence of the trilinear couplings on the mixing angles, we have presented averages over the allowed ranges for these angles. Together with the variances, these show the range of trilinear couplings that can be expected in the two Higgs doublet model with *CP* violation.

There is a region of parameter space of the 2HDM, which we call "*minimal CP violation*," which corresponds to the domain of parameters close to the Higgs sector of the *CP*-conserving minimal supersymmetric standard model. In much of this parameter space there is a considerable enhancement of the trilinear couplings of the two Higgs doublet model as compared with the corresponding trilinear coupling of the SM.

We have computed the radiative corrections to the masses of the Higgs bosons and the trilinear couplings in the one-loop effective potential approximation. The one-loop corrected mass of the lightest neutral Higgs boson can be modified by as much as 20%, whereas the heavier ones are less affected by the radiative corrections. The one-loop corrected trilinear couplings are typically enhanced by the loop effects, but so is the sensitivity to the neutral-sector mixing angles. A similar enhancement due to *CP* violating effects has also been found for the MSSM [50,51].

To a good approximation, decoupling holds in a limited range of parameters, where the model is close to the *CP*-conserving MSSM. In general, however, the heavier states also have a considerable impact on the properties of the lightest Higgs boson. In this sense there is no decoupling in the two Higgs doublet model with *CP* violation.

ACKNOWLEDGMENTS

The research of P. O. has been supported in part by the Research Council of Norway. The work of P. N. P. is supported by the Board of Research in Nuclear Sciences, India under project No. 2007/37/34/BRNS/1970, and by the Council of Scientific and Industrial Research, India under project no. 03(1114)/08/EMR-II. He would like to thank the Abdus Salam ICTP, Trieste, and Department of Physics and Technology, University of Bergen for hospitality where part of this work was done. L. S. is grateful to the Department of Physics and Technology, University of Bergen for its generous hospitality, where part of this work was done, and The Scientific and Technological Research Council of Turkey (TUBITAK) for financial support. It is a great pleasure for L. S. to thank Zekeriya Aydin and Dumus Ali Demir for useful discussions in the early stages of this work.

APPENDIX A: QUARTIC COUPLINGS EXPRESSED IN TERMS OF MASSES

In the 2HDM, with $\mathrm{Im}\lambda_5 \neq 0$, the two masses M_1 and M_2, together with $\boldsymbol{\alpha}$ and $\tan\beta$, determine M_3. The masses will also be related to the quartic couplings of the Higgs potential, via linear relations that can be unambiguously

inverted. It is convenient to distinguish two cases, whether or not λ_6 and λ_7 are nonzero.

1. Approach (A), $\lambda_6 = \lambda_7 = 0$

This case is referred to as approach (A) in the text. Providing also $M_{H^\pm}$ and μ^2, in addition to M_1, M_2 and $\boldsymbol{\alpha}$, all the λ's are determined as follows [17,20]:

$$\lambda_1 = \frac{1}{c_\beta^2 v^2}[c_1^2 c_2^2 M_1^2 + (c_1 s_2 s_3 + s_1 c_3)^2 M_2^2 + (c_1 s_2 c_3 - s_1 s_3)^2 M_3^2 - s_\beta^2 \mu^2], \tag{A1}$$

$$\lambda_2 = \frac{1}{s_\beta^2 v^2}[s_1^2 c_2^2 M_1^2 + (c_1 c_3 - s_1 s_2 s_3)^2 M_2^2 + (c_1 s_3 + s_1 s_2 c_3)^2 M_3^2 - c_\beta^2 \mu^2], \tag{A2}$$

$$\lambda_3 = \frac{1}{c_\beta s_\beta v^2}\{c_1 s_1[c_2^2 M_1^2 + (s_2^2 s_3^2 - c_3^2) M_2^2 + (s_2^2 c_3^2 - s_3^2) M_3^2] + s_2 c_3 s_3 (c_1^2 - s_1^2)(M_3^2 - M_2^2)\} + \frac{1}{v^2}[2M_{H^\pm}^2 - \mu^2], \tag{A3}$$

$$\lambda_4 = \frac{1}{v^2}[s_2^2 M_1^2 + c_2^2 s_3^2 M_2^2 + c_2^2 c_3^2 M_3^2 + \mu^2 - 2M_{H^\pm}^2], \tag{A4}$$

$$\mathrm{Re}\,\lambda_5 = \frac{1}{v^2}[-s_2^2 M_1^2 - c_2^2 s_3^2 M_2^2 - c_2^2 c_3^2 M_3^2 + \mu^2], \tag{A5}$$

$$\mathrm{Im}\lambda_5 = \frac{-1}{c_\beta s_\beta v^2}\{c_\beta[c_1 c_2 s_2 M_1^2 - c_2 s_3 (c_1 s_2 s_3 + s_1 c_3) M_2^2 + c_2 c_3 (s_1 s_3 - c_1 s_2 c_3) M_3^2] + s_\beta[s_1 c_2 s_2 M_1^2 + c_2 s_3 (c_1 c_3 - s_1 s_2 s_3) M_2^2 - c_2 c_3 (c_1 s_3 + s_1 s_2 c_3) M_3^2]\}, \tag{A6}$$

where $c_\beta = \cos\beta$, $s_\beta = \sin\beta$.

While M_3^2 is given in terms of M_1^2, M_2^2, R, and $\tan\beta$, it is more transparent not to substitute for M_3^2 in the expressions (A1)–(A6). These equations are the analogues of those of [52] for the *CP*-conserving 2HDM.

2. Approach (B), $\lambda_6 \neq 0$, $\lambda_7 \neq 0$

In this case, referred to as approach (B) in the text, we take M_1, M_2, M_3, $\boldsymbol{\alpha}$, $M_{H^\pm}$, and μ^2, together with $\mathrm{Im}\lambda_5$, $\mathrm{Re}\lambda_6$, and $\mathrm{Re}\lambda_7$, as the input. In order to keep the notation compact, it is convenient to introduce the following abbreviations:

$$\mathrm{Re}\,\lambda_{345} = \lambda_3 + \lambda_4 + \mathrm{Re}\lambda_5, \tag{A7}$$

$$\mathrm{Re}\,\lambda_{567} = \mathrm{Re}\lambda_5 + \cot\beta\,\mathrm{Re}\lambda_6 + \tan\beta\,\mathrm{Re}\lambda_7. \tag{A8}$$

Then, the λ's can be determined from the following relations:

$$\lambda_1 = \frac{1}{c_\beta^2}\left[\frac{\mathcal{M}_{11}^2 - s_\beta^2 \mu^2}{v^2} - \frac{s_\beta}{2c_\beta}(3c_\beta^2\,\mathrm{Re}\lambda_6 - s_\beta^2\,\mathrm{Re}\lambda_7)\right], \tag{A9}$$

$$\lambda_2 = \frac{1}{s_\beta^2}\left[\frac{\mathcal{M}_{22}^2 - c_\beta^2 \mu^2}{v^2} + \frac{c_\beta}{2s_\beta}(c_\beta^2\,\mathrm{Re}\lambda_6 - 3s_\beta^2\,\mathrm{Re}\lambda_7)\right], \tag{A10}$$

$$\mathrm{Re}\lambda_{345} = \frac{1}{c_\beta s_\beta}\left[\frac{c_\beta s_\beta \mu^2 + \mathcal{M}_{12}^2}{v^2} - \frac{3}{2}(c_\beta^2\,\mathrm{Re}\lambda_6 + s_\beta^2\,\mathrm{Re}\lambda_7)\right], \tag{A11}$$

$$\lambda_4 = \frac{2}{v^2}[\mu^2 - M_{H^\pm}^2] - \mathrm{Re}\lambda_{567}, \tag{A12}$$

$$\mathrm{Re}\,\lambda_5 = \frac{\mu^2 - \mathcal{M}_{33}^2}{v^2} - \frac{1}{2c_\beta s_\beta}(c_\beta^2\,\mathrm{Re}\lambda_6 + s_\beta^2\,\mathrm{Re}\lambda_7), \tag{A13}$$

$$\mathrm{Im}\,\lambda_6 = -\frac{1}{2c_\beta}\left[\frac{2\mathcal{M}_{13}^2}{v^2} + s_\beta\,\mathrm{Im}\lambda_5\right], \tag{A14}$$

$$\mathrm{Im}\,\lambda_7 = -\frac{1}{2s_\beta}\left[\frac{2\mathcal{M}_{23}^2}{v^2} + c_\beta\,\mathrm{Im}\lambda_5\right]. \tag{A15}$$

Invoking Eq. (2.14), the $\mathcal{M}_{ij}^2$ can be expressed in terms of R and the masses M_1, M_2, and M_3.

APPENDIX B: TRILINEAR COUPLING FOR SOME SPECIAL CASES

In order to get a feeling for the trilinear Higgs couplings of the 2HDM, we shall here explicitly write down the two trilinear couplings λ_{111} and λ_{112} for some special cases.

1. The trilinear coupling λ_{111}

We start by writing down Eq. (3.3) explicitly for $\{i, j, k\} = \{1, 1, 1\}$:

$$\lambda_{111} = \sum_{m\le n\le o=1,2,3}^{*} R_{1m}R_{1n}R_{1o}a_{mno} = 3!\{R_{11}^2[R_{11}a_{111} + R_{12}a_{112} + R_{13}a_{113}] + R_{11}[R_{12}^2 a_{122} + R_{12}R_{13}a_{123} + R_{13}^2 a_{133}] + R_{12}[R_{12}^2 a_{222} + R_{12}R_{13}a_{223} + R_{13}^2 a_{233}] + R_{13}^3 a_{333}\}, \tag{B1}$$

where the factor 3! is due to the fact that we here have

couplings to three identical H_1 fields. Substituting for the elements of the rotation matrix, Eq. (2.13), one obtains

$$\begin{aligned}\lambda_{111} = 3!\{&(c_1c_2)^2[c_1c_2a_{111} + s_1c_2a_{112} + s_2a_{113}]\\ &+ c_1c_2[(s_1c_2)^2a_{122} + s_1c_2s_2a_{123} + s_2^2a_{133}]\\ &+ s_1c_2[(s_1c_2)^2a_{222} + s_1c_2s_2a_{223} + s_2^2a_{233}]\\ &+ s_2^3a_{333}\}.\end{aligned} \tag{B2}$$

Let us now consider the case of $\lambda_6 = \lambda_7 = 0$, and substitute for the coefficients a_{mno} from Eq. (3.4). In this case,

$$\begin{aligned}\lambda_{111} = 3\{&c_1c_2c_\beta(c_1^2c_2^2 + s_2^2s_\beta^2)\lambda_1 + s_1c_2s_\beta(s_1^2c_2^2 + s_2^2c_\beta^2)\lambda_2\\ &- 2c_2s_2^2(c_1c_\beta + s_1s_\beta)\,\mathrm{Re}\lambda_{345}\\ &- s_2[(c_2^2 - s_2^2)c_\beta s_\beta + 2c_1s_1c_2^2]\,\mathrm{Im}\lambda_5\}.\end{aligned} \tag{B3}$$

In the limit of no CP violation, with H_1 being odd, we have $c_2 = 0$ [see Eq. (2.15)], and the trilinear coupling simplifies further to

$$\lambda_{111} = 3s_2^3c_\beta s_\beta\,\mathrm{Im}\lambda_5, \tag{B4}$$

with $s_2 = \pm 1$. Similarly, in the limit of no CP violation, with H_3 being odd, we have $s_2 = s_3 = 0$, and obtain the simple expression given in Eq. (3.6a), whereas the limit of no CP violation with H_2 being odd, leads to no further simplification of the expression (B3).

2. The trilinear coupling λ_{112}

We shall again first write Eq. (3.3) explicitly for $\{i, j, k\} = \{1, 1, 2\}$:

$$\begin{aligned}\lambda_{112} &= \sum_{m\le n\le o=1,2,3}^{*} R_{i'm}R_{j'n}R_{k'o}a_{mno} = 2\sum_{m\le n\le o=1,2,3}\{R_{1m}R_{1n}R_{2o} + R_{1m}R_{2n}R_{1o} + R_{2m}R_{1n}R_{1o}\}a_{mno}\\ &= 2\{3R_{11}^2R_{21}a_{111} + R_{11}(R_{11}R_{22} + 2R_{12}R_{21})a_{112} + R_{11}(R_{11}R_{23} + 2R_{13}R_{21})a_{113} + R_{12}(2R_{11}R_{22} + R_{12}R_{21})a_{122}\\ &\quad + [R_{11}(R_{12}R_{23} + R_{13}R_{22}) + R_{12}R_{13}R_{21}]a_{123} + R_{13}(2R_{11}R_{23} + R_{13}R_{21})a_{133} + 3R_{12}^2R_{22}a_{222}\\ &\quad + R_{12}[R_{12}R_{23} + 2R_{13}R_{22}]a_{223} + R_{13}(2R_{12}R_{23} + R_{13}R_{22})a_{233} + 3R_{13}^2R_{23}a_{333}\}.\end{aligned} \tag{B5}$$

If we now substitute for the elements of the rotation matrix, for the coefficients a_{mno}, and set $\lambda_6 = \lambda_7 = 0$, we obtain the result quoted in Eq. (3.6b).

APPENDIX C: DERIVATIVES OF M_ℓ^2

The loop corrections to the trilinear couplings depend on derivatives of the squared masses M_ℓ^2 with respect to the weak fields η_i. In order to obtain these derivatives, a considerable amount of bookkeeping is required. The complication arises from the fact that we allow for CP nonconservation and M_ℓ^2 will thus be determined by the roots of a cubic equation rather than a quadratic one. We start by considering the M_ℓ^2 as functions of the coefficients of the corresponding cubic eigenvalue equation:

$$\frac{\partial M_\ell^2}{\partial\eta_i} = \frac{\partial}{\partial\eta_i}M_\ell^2(a, b, c) \tag{C1}$$

where $M_\ell^2 = \lambda_\ell$ is a solution of

$$\lambda^3 + a\lambda^2 + b\lambda + c = 0, \tag{C2}$$

with field-dependent coefficients:

$$\begin{aligned}a = a(\eta_1, \eta_2, \eta_3), \qquad b = b(\eta_1, \eta_2, \eta_3),\\ c = c(\eta_1, \eta_2, \eta_3).\end{aligned} \tag{C3}$$

These coefficients of the cubic eigenvalue equation are obtained from the derivatives (2.9), where, in contrast to Eq. (2.19), we *do not* set the fields to zero. In terms of the 3×3 mass squared matrix $\mathcal{M}^2$, these coefficients of the cubic equation are given by

$$\begin{aligned}a = -\mathrm{Tr}\mathcal{M}^2, \qquad b = \tfrac{1}{2}\{(\mathrm{Tr}\mathcal{M}^2)^2 - \mathrm{Tr}[(\mathcal{M}^2)^2]\},\\ c = -\det\mathcal{M}^2.\end{aligned} \tag{C4}$$

The derivatives (C1) can thus be split up into simpler entities:

$$\begin{aligned}\frac{\partial}{\partial\eta_i}M_\ell^2(a, b, c) &= \frac{\partial M_\ell^2}{\partial a}\frac{\partial a}{\partial\eta_i} + \frac{\partial M_\ell^2}{\partial b}\frac{\partial b}{\partial\eta_i} + \frac{\partial M_\ell^2}{\partial c}\frac{\partial c}{\partial\eta_i}\\ &= \sum_\alpha \frac{\partial M_\ell^2}{\partial a_\alpha}\frac{\partial a_\alpha}{\partial\eta_i},\end{aligned} \tag{C5}$$

where we have introduced the collective notation

$$a_\alpha = \{a, b, c\}. \tag{C6}$$

The higher derivatives can likewise be written as

$$\frac{\partial^2 M_\ell^2}{\partial\eta_i\partial\eta_j} = \sum_\alpha\Big[\sum_\beta \frac{\partial^2 M_\ell^2}{\partial a_\alpha\partial a_\beta}\frac{\partial a_\alpha}{\partial\eta_i}\frac{\partial a_\beta}{\partial\eta_j} + \frac{\partial M_\ell^2}{\partial a_\alpha}\frac{\partial^2 a_\alpha}{\partial\eta_i\partial\eta_j}\Big], \tag{C7}$$

$$\frac{\partial^3 M_\ell^2}{\partial\eta_i\partial\eta_j\partial\eta_k} = \sum_\alpha\Big\{\sum_\beta\Big[\sum_\gamma \frac{\partial^3 M_\ell^2}{\partial a_\alpha\partial a_\beta\partial a_\gamma}\frac{\partial a_\alpha}{\partial\eta_i}\frac{\partial a_\beta}{\partial\eta_j}\frac{\partial a_\gamma}{\partial\eta_k} + \frac{\partial^2 M_\ell^2}{\partial a_\alpha\partial a_\beta}\Big(\frac{\partial^2 a_\alpha}{\partial\eta_i\partial\eta_j}\frac{\partial a_\beta}{\partial\eta_k} + \frac{\partial^2 a_\alpha}{\partial\eta_j\partial\eta_k}\frac{\partial a_\beta}{\partial\eta_i} + \frac{\partial^2 a_\alpha}{\partial\eta_k\partial\eta_i}\frac{\partial a_\beta}{\partial\eta_j}\Big)\Big] + \frac{\partial M_\ell^2}{\partial a_\alpha}\frac{\partial^3 a_\alpha}{\partial\eta_i\partial\eta_j\partial\eta_k}\Big\}. \tag{C8}$$

1. Cubic equation

In order to obtain the derivatives of M_ℓ^2 with respect to the a_α that enter Eqs. (C5), (C7), and (C8), we start by solving the cubic equation (C2) in terms of the following notation. Let

$$q = \tfrac{1}{3}b - \tfrac{1}{9}a^2, \qquad r = \tfrac{1}{6}(ab - 3c) - \tfrac{1}{27}a^3 \tag{C9}$$

and

$$s_1 = [r + \Delta]^{1/3}, \qquad s_2 = [r - \Delta]^{1/3}, \tag{C10}$$

with the discriminant

$$\Delta^2 \equiv q^3 + r^2. \tag{C11}$$

Then the solutions can be written as

$$\begin{aligned} m_1^2 &= (s_1 + s_2) - \frac{a}{3}, \\ m_2^2 &= -\frac{1}{2}(s_1 + s_2) - \frac{a}{3} + \frac{i\sqrt{3}}{2}(s_1 - s_2), \\ m_3^2 &= -\frac{1}{2}(s_1 + s_2) - \frac{a}{3} - \frac{i\sqrt{3}}{2}(s_1 - s_2), \end{aligned} \tag{C12}$$

where the $\{m_1, m_2, m_3\}$ refer to the set of masses $\{M_1, M_2, M_3\}$, but not necessarily ordered. In the one-loop contribution to the potential (4.2), only a sum over ℓ enters, the order plays no role.

We recall that the coefficients $a_\alpha = \{a, b, c\}$ that enter in the cubic eigenvalue equation (C2) depend on the weak fields η_i. In the solutions (C12), this dependence can be accessed via a, s_1 and s_2. It is thus convenient to write (C12) more compactly as

$$m_\ell^2 = -\frac{a}{3} + \sum_{r=1}^{2} A_{\ell r} s_r, \tag{C13}$$

from which it follows that

$$\frac{\partial m_\ell^2}{\partial a_\alpha} = -\frac{1}{3}\delta_{\alpha 1} + A_{\ell r}\frac{\partial s_r}{\partial a_\alpha}. \tag{C14}$$

Likewise, the higher derivatives are given by

$$\begin{aligned} \frac{\partial^2 m_\ell^2}{\partial a_\alpha\partial a_\beta} &= A_{\ell r}\frac{\partial^2 s_r}{\partial a_\alpha\partial a_\beta}, \\ \frac{\partial^3 m_\ell^2}{\partial a_\alpha\partial a_\beta\partial a_\gamma} &= A_{\ell r}\frac{\partial^3 s_r}{\partial a_\alpha\partial a_\beta\partial a_\gamma}. \end{aligned} \tag{C15}$$

It remains to obtain the derivatives of s_r with respect to a_α. For this purpose, it is useful to think of s_r as a function of the q and r of Eqs. (C9)–(C11). The first derivatives are given by

$$\frac{\partial s_r}{\partial a_\alpha} = \frac{\partial s_r}{\partial q}\frac{\partial q}{\partial a_\alpha} + \frac{\partial s_r}{\partial r}\frac{\partial r}{\partial a_\alpha} = \frac{\partial s_r}{\partial Q^s}\frac{\partial Q^s}{\partial a_\alpha}, \tag{C16}$$

where we collectively refer to q and r as

$$Q^s = \{q, r\}. \tag{C17}$$

In this notation, the higher derivatives can be written as

$$\frac{\partial^2 s_r}{\partial a_\alpha\partial a_\beta} = \frac{\partial^2 s_r}{\partial Q^s\partial Q^t}\frac{\partial Q^s}{\partial a_\alpha}\frac{\partial Q^t}{\partial a_\beta} + \frac{\partial s_r}{\partial Q^s}\frac{\partial^2 Q^s}{\partial a_\alpha\partial a_\beta}, \tag{C18}$$

and

$$\frac{\partial^3 s_r}{\partial a_\alpha\partial a_\beta\partial a_\gamma} = \frac{\partial^3 s_r}{\partial Q^s\partial Q^t\partial Q^u}\frac{\partial Q^s}{\partial a_\alpha}\frac{\partial Q^t}{\partial a_\beta}\frac{\partial Q^u}{\partial a_\gamma} + \frac{\partial^2 s_r}{\partial Q^s\partial Q^t} \times\Big[\frac{\partial^2 Q^s}{\partial a_\alpha\partial a_\beta}\frac{\partial Q^t}{\partial a_\gamma} + \frac{\partial^2 Q^s}{\partial a_\beta\partial a_\gamma}\frac{\partial Q^t}{\partial a_\alpha} + \frac{\partial^2 Q^s}{\partial a_\gamma\partial a_\alpha}\frac{\partial Q^t}{\partial a_\beta}\Big] + \frac{\partial s_r}{\partial Q^s}\frac{\partial^3 Q^s}{\partial a_\alpha\partial a_\beta\partial a_\gamma}. \tag{C19}$$

Finally, the various derivatives $\partial Q^r/\partial a_\alpha$ are given by

$$\frac{\partial q}{\partial a} = -\frac{2}{9}a, \qquad \frac{\partial r}{\partial a} = \frac{1}{6}b - \frac{1}{9}a^2, \qquad \frac{\partial q}{\partial b} = \frac{1}{3}, \qquad \frac{\partial r}{\partial b} = \frac{1}{6}a, \qquad \frac{\partial q}{\partial c} = 0, \qquad \frac{\partial r}{\partial c} = -\frac{1}{2}, \tag{C20}$$

$$\frac{\partial s_1}{\partial q} = \frac{Q^2}{2\Delta\sqrt[2/3]{r + \Delta}}, \qquad \frac{\partial s_1}{\partial r} = \frac{1 + \frac{r}{\Delta}}{3\sqrt[2/3]{r + \Delta}}, \qquad \frac{\partial s_2}{\partial q} = -\frac{Q^2}{2\Delta\sqrt[2/3]{r - \Delta}}, \qquad \frac{\partial s_2}{\partial r} = \frac{1 - \frac{r}{\Delta}}{3\sqrt[2/3]{r - \Delta}} \tag{C21}$$

$$\frac{\partial s_1}{\partial a} = \frac{-a}{9}\frac{Q^2}{\Delta\sqrt[2/3]{r+\Delta}} + \frac{1+\frac{r}{\Delta}}{3\sqrt[2/3]{r+\Delta}}\left(\frac{1}{6}b - \frac{1}{9}a^2\right),$$
$$\frac{\partial s_1}{\partial b} = \frac{1}{6}\frac{Q^2}{\Delta\sqrt[2/3]{r+\Delta}} + \frac{a}{18}\frac{1+\frac{r}{\Delta}}{\sqrt[2/3]{r+\Delta}},$$
$$\frac{\partial s_1}{\partial c} = -\frac{1}{6}\frac{1+\frac{r}{\Delta}}{\sqrt[2/3]{r+\Delta}},$$
$$\frac{\partial s_2}{\partial a} = \frac{a}{9}\frac{Q^2}{\Delta\sqrt[2/3]{r-\Delta}} + \frac{1-\frac{r}{\Delta}}{3\sqrt[2/3]{r-\Delta}}\left(\frac{1}{6}b - \frac{1}{9}a^2\right), \qquad \text{(C22)}$$
$$\frac{\partial s_2}{\partial b} = -\frac{1}{6}\frac{Q^2}{\Delta\sqrt[2/3]{r-\Delta}} + \frac{a}{18}\frac{1-\frac{r}{\Delta}}{\sqrt[2/3]{r-\Delta}},$$
$$\frac{\partial s_2}{\partial c} = -\frac{1}{6}\frac{1-\frac{r}{\Delta}}{\sqrt[2/3]{r-\Delta}}.$$

[1] F. Englert and R. Brout, Phys. Rev. Lett. **13**, 321 (1964); P. W. Higgs, Phys. Rev. Lett. **13**, 508 (1964); Phys. Rev. **145**, 1156 (1966).

[2] H. P. Nilles, Phys. Rep. **110**, 1 (1984); H. E. Haber and G. L. Kane, Phys. Rep. **117**, 75 (1985); R. Barbieri, Riv. Nuovo Cimento Soc. Ital. Fis. **11N4**, 1 (1988); M. Drees, R. Godbole, and P. Roy, *Theory and Phenomenology of Sparticles: An Account of Four-dimensional $N = 1$ Supersymmetry in High Energy Physics* (World Scientific, Hackensack, USA, 2004).

[3] J. F. Gunion, H. E. Haber, G. L. Kane, and S. Dawson, *The Higgs Hunter's Guide* (Addison-Wesley, Reading, 1990).

[4] G. Weiglein *et al.* (LHC/LC Study Group), Phys. Rep. **426**, 47 (2006).

[5] E. Accomando *et al.* (ECFA/DESY LC Physics Working Group), Phys. Rep. **299**, 1 (1998).

[6] A. Djouadi, H. E. Haber, and P. M. Zerwas, Phys. Lett. B **375**, 203 (1996); P. Osland and P. N. Pandita, Phys. Rev. D **59**, 055013 (1999); arXiv:hep-ph/9911295; arXiv:hep-ph/9902270; D. J. Miller and S. Moretti, Eur. Phys. J. C **13**, 459 (2000).

[7] J. A. Aguilar-Saavedra *et al.* (ECFA/DESY LC Physics Working Group), arXiv:hep-ph/0106315.

[8] A. Arhrib, R. Benbrik, and C. W. Chiang, Phys. Rev. D **77**, 115013 (2008).

[9] G. Ferrera, J. Guasch, D. Lopez-Val, and J. Sola, Phys. Lett. B **659**, 297 (2008).

[10] T. D. Lee, Phys. Rev. D **8**, 1226 (1973).

[11] S. Weinberg, Phys. Rev. Lett. **37**, 657 (1976).

[12] G. C. Branco and M. N. Rebelo, Phys. Lett. **160B**, 117 (1985); J. Liu and L. Wolfenstein, Nucl. Phys. **B289**, 1 (1987); S. Weinberg, Phys. Rev. D **42**, 860 (1990); Y. L. Wu and L. Wolfenstein, Phys. Rev. Lett. **73**, 1762 (1994).

[13] E. Accomando *et al.*, arXiv:hep-ph/0608079.

[14] N. Cabibbo, Phys. Rev. Lett. **10**, 531 (1963); M. Kobayashi and T. Maskawa, Prog. Theor. Phys. **49**, 652 (1973).

[15] S. Kanemura, S. Kiyoura, Y. Okada, E. Senaha, and C. P. Yuan, Phys. Lett. B **558**, 157 (2003).

[16] S. L. Glashow and S. Weinberg, Phys. Rev. D **15**, 1958 (1977).

[17] A. W. El Kaffas, P. Osland, and O. M. Ogreid, Nonlinear Phenomena in Complex Systems **10**, 347 (2007).

[18] W. Khater and P. Osland, Acta Phys. Pol. B **34**, 4531 (2003).

[19] W. Khater and P. Osland, Nucl. Phys. **B661**, 209 (2003).

[20] A. W. El Kaffas, W. Khater, O. M. Ogreid, and P. Osland, Nucl. Phys. **B775**, 45 (2007).

[21] A. W. El Kaffas, P. Osland, and O. M. Ogreid, Phys. Rev. D **76**, 095001 (2007).

[22] A. Barroso, P. M. Ferreira, and R. Santos, Phys. Lett. B **652**, 181 (2007).

[23] R. Barbieri, L. J. Hall, and V. S. Rychkov, Phys. Rev. D **74**, 015007 (2006).

[24] S. Y. Choi and J. S. Lee, Phys. Rev. D **61**, 015003 (1999).

[25] M. Carena, J. Ellis, S. Mrenna, A. Pilaftsis, and C. E. Wagner, Nucl. Phys. **B659**, 145 (2003).

[26] V. D. Barger, M. S. Berger, A. L. Stange, and R. J. N. Phillips, Phys. Rev. D **45**, 4128 (1992).

[27] J. F. Gunion and H. E. Haber, Phys. Rev. D **67**, 075019 (2003).

[28] W. Hollik and S. Penaranda, Eur. Phys. J. C **23**, 163 (2002).

[29] A. Dobado, M. J. Herrero, W. Hollik, and S. Penaranda, Phys. Rev. D **66**, 095016 (2002).

[30] N. G. Deshpande and E. Ma, Phys. Rev. D **18**, 2574 (1978); S. Nie and M. Sher, Phys. Lett. B **449**, 89 (1999); S. Kanemura, T. Kasai, and Y. Okada, Phys. Lett. B **471**, 182 (1999).

[31] S. Kanemura, T. Kubota, and E. Takasugi, Phys. Lett. B **313**, 155 (1993).

[32] A. G. Akeroyd, A. Arhrib, and E. M. Naimi, Phys. Lett. B **490**, 119 (2000); A. Arhrib, arXiv:hep-ph/0012353.

[33] I. F. Ginzburg and I. P. Ivanov, arXiv:hep-ph/0312374; Phys. Rev. D **72**, 115010 (2005).

[34] P. Koppenburg *et al.* (Belle Collaboration), Phys. Rev. Lett. **93**, 061803 (2004); B. Aubert *et al.* (*BABAR* Collaboration), Phys. Rev. D **72**, 052004 (2005); B. Aubert (*BABAR* Collaboration), Phys. Rev. D **77**, 051103(R) (2008).
[35] E. Barberio *et al.* (Heavy Flavor Averaging Group (HFAG)), arXiv:hep-ex/0603003.
[36] M. Misiak *et al.*, Phys. Rev. Lett. **98**, 022002 (2007).
[37] K. Ikado *et al.*, Phys. Rev. Lett. **97**, 251802 (2006); T. E. Browder, Nucl. Phys. B, Proc. Suppl. **163**, 117 (2007); B. Aubert (*BABAR* Collaboration), arXiv:hep-ex/0608019.
[38] W. S. Hou, Phys. Rev. D **48**, 2342 (1993); Y. Grossman and Z. Ligeti, Phys. Lett. B **332**, 373 (1994); Y. Grossman, H. E. Haber, and Y. Nir, Phys. Lett. B **357**, 630 (1995).
[39] J. Urban, F. Krauss, U. Jentschura, and G. Soff, Nucl. Phys. **B523**, 40 (1998).
[40] W. M. Yao *et al.* (Particle Data Group), J. Phys. G **33**, 1 (2006).
[41] A. Denner, R. J. Guth, W. Hollik, and J. H. Kuhn, Z. Phys. C **51**, 695 (1991).
[42] S. Bertolini, Nucl. Phys. **B272**, 77 (1986).
[43] S. Schael *et al.* (ALEPH Collaboration, DELPHI Collaboration, L3 Collaboration, OPAL Collaboration, SLD Collaboration, LEP Electroweak Working Group, SLD Electroweak Group, and SLD Heavy Flavour Group), Phys. Rep. **427**, 257 (2006).
[44] W. Grimus, L. Lavoura, O. M. Ogreid, and P. Osland, J. Phys. G **35**, 075001 (2008).
[45] Y. Okada, M. Yamaguchi, and T. Yanagida, Prog. Theor. Phys. **85**, 1 (1991); J. R. Ellis, G. Ridolfi, and F. Zwirner, Phys. Lett. B **257**, 83 (1991); H. E. Haber and R. Hempfling, Phys. Rev. Lett. **66**, 1815 (1991).
[46] S. W. Ham, S. K. Oh, E. J. Yoo, C. M. Kim, and D. Son, Phys. Rev. D **68**, 055003 (2003).
[47] S. R. Coleman and E. Weinberg, Phys. Rev. D **7**, 1888 (1973).
[48] S. Weinberg, Phys. Rev. Lett. **29**, 1698 (1972); Phys. Rev. D **7**, 2887 (1973).
[49] J. M. Gerard and M. Herquet, Phys. Rev. Lett. **98**, 251802 (2007).
[50] M. N. Dubinin and A. V. Semenov, Eur. Phys. J. C **28**, 223 (2003).
[51] Yu. P. Philippov, Phys. At. Nucl. **70**, 1288 (2007).
[52] R. Casalbuoni, D. Dominici, F. Feruglio, and R. Gatto, Nucl. Phys. **B299**, 117 (1988).